Journal Name

ARTICLE

Progress in biomimetic leverages for marine antifouling by nanocomposite coatings

-Received 00th January 20xx,
Accepted 00th January 20xx

DOI: 10.1039/x0xx00000x
www.rsc.org/

M. S. Selim [a,b], S. A. El-Safty [a]*, M. A. Shenashen [a], S. A. Higazy [b], A. Elmarakbi [c]

Because of the environmental and economic casualties of biofouling on the maritime navigation, modern researches have been devoted to module advanced nanoscale composites in controlled development of effective marine antifouling self-cleaning surfaces. Natural biomimetic surface merits of micro/nano-roughness and minimized free-energy characteristics would motivate the dynamic fabrication of superhydrophobic antifouling surfaces. This review provides an architectural panorama of the biomimetic antifouling designs and their key leverages to broaden horizons in the controlled fabrication of nanocomposite building-blocks as force-driven marine antifouling models. As primary antifouling designs, understanding the key function of surface geometry, heterogeneity, superhydrophobicity, and complexity of polymer/nanofiller composite building blocks on fouling resistance systems is crucial. This review also discussed a wide-range of fouling-release coating systems that satisfy the growing demand in sustainable future environment. For instance, the integration of block, segmented copolymer-based coatings, and inorganic-organic hybrid nanofillers enhanced antifouling model properties with mechanical, superhydrophobic, chemically-inert and robust surfaces. These nano-scale antifouling systems offered surfaces with minimized free-energy, micro/nano-roughness, anisotropic heterogeneity superior hydrophobicity, tunable non-wettability, antibacterial efficiency, and mechanical robustness. The confined fabrication of nanoscale orientation, configuration, arrangement, and direction along architectural composite building-blocks would enable an excellent air-entrapping along interfacial surface grooves, and interfaces, which optimized the antifouling coating surfaces for long-term durability. This review provided dexterous evidence of the effect of the structurally folded nanocomposites, nano-filler tectonics, and building-blocks on creation of outstanding superhydrophobicity, self-cleaning surfaces, and potential antifouling coatings. Development of modern research gateways is a candidate for sustainable future of antifouling coatings.

Keywords: Marine antifouling, biomimetic surface, superhydrophobicity, hybrid nanofillers, quaternary nanocomposites, long-term durability.

1. Introduction

For maritime navigation, biofouling is a terrifying nightmare and dynamic problems in adverse environmental effects, industrial impacts, and capital costs.[1] Shipping accounts are represented about 90% of the worldwide trade. The friction drags and fuel consumption increase by fouling layers, which reduce the hydrodynamic performance and then the overall velocity of the ship.[1] Several negative economic and ecological impacts such as increase shipping costs and environmental hazards are produced by fouling adhesion.[2] The fouling adhesion to the hull plays a key role to enhance the vessel's drag resistance and then decrease its velocity.[3] This mechanistic formation of biofouling contributes to an emission of harmful gases (CO_2, SO_x. and NO_x) and increasing of fuel consumption.[2,3] The latter leads to enhance the cost-effective of shipping industry approximately ~ $1 billion (dollar)/annually.[1,2]

Intensive efforts and innovative strategies to improve the fouling prevention of ship hulls have a particular interest.[2] The international prohibition followed the use of biocidal antifouling AF paints has directed recent researches toward environmental-friendly coatings, particularly the fouling-release (FR) coatings.[4] These FR coatings are non-stick, non-toxic surfaces with high mobility and fouling anti-adhesion mechanism. The FR resins, including polysiloxane and fluoro-based polymers, showed effective functions as easy-cleaning systems through physical hindering behaviour of the settled biofouling.[4] Polysiloxanes have prominent matrix for FR coating functions compared with fluoropolymers.[4] The strong binding of fluorine atoms inherits high stiffness in the fluoropolymer structures, making the structural rotation along the its matrix backbone more difficult, and thus prevents the easy-release of biofouling attachments.[5]

Nanomaterials play essential functions in wide-spread applications from environmental remediation and sustainable healthcare future to green energy, affording eco-friendly and comfortable life. [6,7] Polydimethylsiloxane (PDMS)-based coatings offered non-toxicity, water and biofouling repellency and thermal resistance polymers. These PDMS building blocks featured flexible structure, hydrophobic surface, reduced surface tension, and easy FR systems.[8] PDMS's fouling-prevention can be enhanced by well-defined distribution of nano-scale filler architectures along PDMS matrices.[9] Superhydrophobic FR surfaces are cost-saving trends for marine durable coatings. Because of their outstanding fouling-prevention features, natural superhydrophobic surfaces have driven the innovation research for fabrication of advanced self-cleaning nanocomposites.[10] Butterflies wings, cabbage leaves, and Indian cress plants are good examples of natural superhydrophobic surfaces.[11] Lotus plant leaves (Nelumbo nucifera) are the most famous hydrophobic self-cleaning examples due to the formation of *"Lotus Effect"* ultrahydrophobicity.[12] Surface micro-roughness of epicuticular wax is formed with 20-40 µm protruding ganglion.[13] Superhydrophobic surfaces exhibited an ultrahigh contact angle > 150° with reduced contact angle hysteresis of <5°. These features were formed due to the low free energy and micro-/nano-binary rough topology of the surfaces.[14]

To engineer advanced antifouling and self-cleaning coatings, selection of nanomaterials-based ultrahydrophobic surfaces and tectonic architectures

[a] National Institute for Materials Science (NIMS), 1-2-1 Sengen, Tsukuba-shi, Ibaraki-ken 305-0047, Japan.
E-mail: sherif.elsafty@nims.go.jp
https://samurai.nims.go.jp/profiles/sherif_elsafty
[b] Petroleum Application Department, Egyptian Petroleum Research Institute, Nasr City 11727, Cairo (Egypt).
[c] Department of Mechanical & Construction Engineering, Faculty of Engineering and Environment, Northumbria University, Newcastle upon Tyne, NE1 8ST, UK.

that have outstanding physical, chemical, and biological properties is crucial.[15] Nano-scale structures featured high surface area to volume ratio, cost-effectiveness, compatibility with the polymeric segments lead to improved bonding strength of the resultant composite building blocks.[16-20] The fabrication of superhydrophobic surfaces was successfully achieved through well-dispersion, and excellent compatibility, and stability of the matrix-nanomaterial/polymer interaction. Surface rough-topology and superhydrophobicity can be enhanced by dominating the structures of polymer and nanofillers.[21] The high solid–liquid interface properties can increase both surface roughness and its hydrophobicity. A pool-on-surface can be formed by the air trapping within the grooves and ridges that allocated naturally on rough material surfaces under water dropping process. This structurally-superhydrophobic surface-based nanomaterials can improve self-cleaning coatings (since air exhibits water contact angle (WCA of 180˚).[25] Micro-/nano-roughness and minimized free energy of the coated film are thus responsible for superhydrophobicity.[22]

Superhydrophobicity provides a pathway toward the protection of sensitive surface characteristics.[23] Etching, lithography, biomimetic and stamping processes were applied to fabricate superhydrophobic nano-surfaces. In addition, a facile method of nanoparticles (NPs) dispersion in a hydrophobic polymer matrix would lead to control the surface superhydrophobicity.[24] Modifying the PDMS resin using epoxy, polyurethane, and fluorinated units with hybrid nanofillers can improve the component features and produce ternary and quaternary nanocomposites.

As an effective coating technique for fouling prevention, an insertion of different nanofillers (including metal oxides, noble metals, and graphene-based materials) can increase the resistance against micro-organism attacks.[25] Nanomaterials such as ZnO nanorods (NRs), Cu_2O nanocubes, titania nanospheres, Ag@SiO_2, β-MnO_2 NRs, carbon nanotubes (CNTs), and graphene (G) materials are applicable in feasible and advanced development of marine antifouling (Figure 1).[26,27]

Figure 1

Graphene-materials such as graphene oxide (GO) and reduced GO (rGO) exhibited ultrahigh mechanical stiffness, high conductivity, extra-ordinary electronic transportation, and ultrahigh thermal conductivity; as a result of their two-dimensional (2D) crystals.[28] The ultimate tensile strength (130 GPa), and the electrical and thermal conductivity characteristics of graphene are greater than the pristine CNTs.[29] The graphene materials also exhibited extra-large specific surface area (2630 m^2/g) with the capability of adjusting their underlying attitude using polymer composite hybrids for potential applications.[30] The hydrophobic performance could be enhanced by chemical and surface modifications that alter microstructure building blocks of graphene.[31] For instance, 3D graphene foams were fabricated by using a nickel skeleton through chemical vapour deposition technique (CVD). Coated film of 3D graphene foam showed superhydrophobic feature with WCA of 150˚.[32] Porous composites of polyvinylidine fluoride (PVDF)/graphene was fabricated with WCA of 153˚.[33] However, in situ polymerization and carbonization methods were used to control superhydrophobicity, and stiffness of rGO/glassy carbon-film composites.[34] Various synthetic techniques including solution casting, in-situ and sol–gel were employed to develop controlled superhydrophobic nanocomposite structures.[35]

Considering the essential demands of eco-friendly, non-toxic and robust marine antifouling coating, the development of advanced silicone copolymer coating enriched with hybrid nanofillers may provide economic and environmentally friendly alternatives. The control over surface functionality, geometrical morphology, nanoscale size, active site function of nanocomposites was intrinsically improved by embedding and distribution of nanofillers into homo- and co-polymer matrices. Together, the synergetic strategy supported the engineering ternary and quaternary nanocomposites, leading to form superhydrophobic slippery antifouling surface and reduced free energy.[36] In this review, we also provided the key function of nanocomposite coatings that represented a mature rostrum to develop robust superhydrophobic self-cleaning and FR structures for the maritime navigation.

2. Maritime biofouling and its adverse impacts

Biofouling represents a fast, dynamic, and complicated problem with several forefronts in the shipping industry. Marine biofouling is associated with the unwanted settlements of biotic and abiotic compounds, micro and/or macro-organisms, plants and animals. [1, 37, 38] Biofouling strains are classified into (i) biofilm labelled as conditioned film, (ii) microfouling, and (iii) macrofouling, as illustrated in Figure 2A.[39] These fouling organisms can be attached through three main adhesion stages as follows:

The first fouling organism is the biofilm, which is termed as conditioned film and formed from the collected microbes on natural polymers. These polymers are secreted by micro-organisms expressed by extracellular polymeric substances (EPS).[40-42]

The second fouling organism is the microfouling, which includes two stages; (i) the primary colonization, where the colonizers included diatoms and bacteria, can be adsorbed physically over the conditioned film and then it can be easily detached[43]; and (ii) secondary colonization, where the colonizers included protozoa and spores of macroalgal spores, can form microfilm with a mass that is increasing nonlinearly.

The third fouling organism is the macrofouling. Due to its large contribution to the ship's hydrodynamic weight, macrofouling has a great concern.[44]

Marine biofouling is a nightmare which revealed the loss of billions of dollars annually in shipping industry. The shipping is the prime facilitator (nearly 90%) of the worldwide trading. [1] Several ecological and economic problems such as increase environmental hazards and shipping costs are produced by fouling adhesion, as illustrated in Figure 2A. When the hull surface was fouled through fouling attachments, sequent features could be found as follows; (i) the increased drag resistance, (ii) the minimized ship velocity with the loss of manoeuvrability, (iii) the maximized fuel consumption, and (iv) the increased emission rate and amount of pollutant gases (including NO_x, CO_2, and SO_x) to environment. As a result, the dry-docking intervals were shortened and the total voyage costs are increased.[45, 46]

As top hedge impacts, approximately €200 billion is wasted and 60,000 people are died annually because of the toxic emissions.[47] These negative impacts have pushed the advanced technology towards the development concerns of antifouling nanocomposite coatings. Previously, inhibition of fouling organisms was performed through biocidal coatings, however their poisonous impacts affected strictly the non-target animals such as fishes and dolphins.[48] Also, these antifouling coatings suffered from equipment maintenance, and the corrosion of metallic surfaces.[49] Fouling also could damage the paint coatings that are used to protect the surfaces and form rusting.[50] The toxicity of marine water was caused by biocidal antifouling coating; which wasted daily much more time because of the leaching effect. Such reduction of coating film increased the corrosion factors and maintenance costs. [51] The global market is worth billions of dollars annually because of fouling problems and biocidal coatings.[52] These biofouling impacts have driven modern research toward ecological, economic, and elastomeric FR coating (especially the silicone-based composites) for ship hull coatings. These non-toxic and non-leachant composites represent economic coatings for marine antifouling. Furthermore, natural superhydrophobic surfaces have driven the development of novel superhydrophobic, and biomimetic antifouling nano-surfaces with controlled topological structures.[53]

Figure 2

3. Antifouling strategic techniques

Because of the economic and ecological problems of fouling, engineers and scientists are devoted to develop antifouling strategies by chemical methods and engineered instruments. There are two principal approaches to solve the fouling problems; non-coating and coating techniques.[54]

3.1. Non-coating technique

Previously, numerous non-coating fouling prevention techniques were developed such as electrical, irradiation and sonochemical techniques.[55, 56] Ultra-sonic transducers installed inside the hull emit pulses, which restrain the active cell functions for enhanced early-stage fouling. The ultra-sonic transducers must be kept switched on to be effective, except when the vessel is moving at speed. The types of hull construction and structural materials used affect the transmission. The ultrasonic pulses-some types of sandwich core construction would absorb a high amount of the ultrasonic energy, thereby reducing its effectiveness. Ultrasonic vibration techniques were expensive and insufficient prevention methods for the ship hull.[57] Also, the

cleaning of the surface was an essential approach through either the water jet technology or mechanical scrubbing. In general, the non-coating techniques were less effective, more expensive and less practical, but sometimes useful only for small boats.[58,59] Ultrasonic vibration techniques were expensive and insufficient prevention methods for the large vessels.

3.2. Antifouling coatings as promising eco-friendly techniques

As an effective technique, antifouling coating has been widely applied. In the past, biocidal antifouling coating were used**.** Over 2000 years, wax and tar were employed for fouling prevention on the marine ships. The history of the development of antifouling technologies was very old as mentioned in Table 1.[59-67] The problem of marine fouling was considered from the ancient dates by many civilizations (such as Carthaginians, Phoenicians, Greeks, Romans, Plutarch…etc).[59,60] Along with that the advent of iron ships and the subsequent corrosion, biocidal antifouling paints were used. An efficient TBT (tributyltin)-copolymer was functionally developed as a self-polishing coating in the late 1970s.[59, 60] This early-used technique caused fouling toxicity using toxicants (e.g., biocides). However, this technique provided smooth and hydrodynamic surfaces, and reduced the fuel consumption. The building blocks of TBT-based coatings were formulated by using methacrylic or acrylic copolymers, and the biocides, which could be hydrolysed in the marine water. Figure 2B showed an example of the leaching of a copolymer methyl methacrylate and TBT-acrylate. The released toxicants of TBT in the seawater could attack the microorganisms.[43] This coating design provided various advantages, such as smooth hydrodynamic profile during sailing, decreased fuel consumption, and constant biocide release rates over time. The TBT-based coatings are well-known as the most powerful biocidal antifouling coating. However their negative side effects on non-target organisms have driven modern regulates for the International Maritime Organization's (IMO) prohibition use in 2008.[68] Since the harmful effects of tin-based fouling-prevention coatings have been approved, the tin-free materials coatings were developed using other toxic biocides (especially Cu^{2+}) as alternatives.[69] However, serious obstacle and mysterious fate caused by their toxic effects and release rates were restricted their wide-applications. Another disadvantage was that many fouling strains were tolerant to such coatings. As such, copper antifouling paints were formulated with additional “booster” biocides (including diuron and Irgarol 1051).[70] Such biocides negatively affect the rate of the growth of the photosynthetic organisms, leading to prohibited utilization in some countries. For example, Australia and Netherlands banned Irgarol 1051, and diuron, respectively; however, Denmark banned both of them.[71]

Natural marine compounds are eco-friendly antifouling alternatives, which were replaced effectively the biocidal antifouling coating. Upon insertion of natural marine compounds in the antifouling building blocks, they could prevent fouling attachments.[72,73] This idea was gotten after noticing that the marine organisms were used these marine compounds to prevent fouling. These compounds included amino-acids, heterocyclics, fatty acids, acerogenins and halogenated compounds.[73] The key mechanism of these natural compounds in the antifouling building blocks included (i) attachment prevention, (ii) growth inhibition, (iii) negative chemotaxis upgrading, (iv) fouling repellence, and (v) organisms' death. However, these compounds were eco-friendly and effective solutions, but applying of these compounds in high performance of antifouling system was limited due to the following key facts;[74]

i. it was difficult to incorporate the natural biocides into the active site inside the matrix of the coating,
ii. it was hard to release such compounds in a well-behaved way,
iii. their registration procedures were expensive and taking awfully long time, and
iv. it was difficult to produce these compounds in large scale manufactures.

Therefore, to control the environmentally eco-friendly AF future, the demand of nontoxic antifouling coating especially the silicone FR coatings is grown very rapidly. These silicone FR surfaces produce low surface free energy (SFE), non-stick coating without leaching properties. Indeed, the silicone FR building blocks represent the most promising eco-friendly alternatives.

Table 1

To date, FR paints especially those based on silicone (Sylgard 184 and RTV11) matrices were developed. In 2004, studying the morphological structure of lotus leaves by scanning electron microscope (SEM) images inspired the suggested design of Sharklet AF™ self-cleaning antifouling surface, as an effective biomimetic self-cleaning suture. A series of polymer nanocomposites was designed to mimic lotus leaves and shark skin for antifouling applications. Many copolymers, nanocomposites and hybrid nanofiller/composites were designed for enhancing the self-cleaning and antifouling effectiveness.

4. Biomimetic antifouling strategies

Studying the biological systems in terms of function and structure is a model to engineered material tectonics, hierarchy architectures, surfaces, designs, and machines, namely called biomimetics.[75] Such biological systems may lead to develop FR coating materials and technologies. A key FR technology is based on the fabrication of biomimetic surface with micro/nano structure for fouling-prevention in the marine environment. As a result, it is crucial to shed lights on the approach and accuracy for developing bio-replicated structures with multi-scale structures for fouling-prevention. One of a facile and applicable method is to design artificial structures by using polymers, nanofillers, and nanocomposites through biomimetic technology. [76,77]

A biomimetic surface was developed for drag-reduction and marine self-cleaning by Han et al.[78] Although many organisms such as Sharks, Dolphins, and Crabs live in the marine water, they are rarely fouled as their skins prevent fouling adhesion. As a result, studying the microstructure, morphological, physical and physiological properties of these organisms is inevitable for mimicking their functions in analogously artificial surfaces.[79]

4.1. Mimicking the Lotus surfaces in antifouling coatings

Superhydrophobic surfaces were established cost-effective and eco-friendly solutions for different fields such as antifouling coatings, anti-icing, anti-corrosion, and textiles. Lotus plant leaves (Nelumbo nucifera) are the most famous superhydrophobicity and exemplary self-cleaning surfaces, in which the *"Lotus Effect"* was obvious.[14] Surface micro-roughness of epicuticular wax is formed with 20-40 µm protruding ganglion.[80] Superhydrophobic surfaces formed with WCAs more than 150°, and at a reduced contact angle hysteresis (CAH <5°). The leaves of lotus plant possess a highly stable superhydrophobic surface compared with many other plants that exhibit WCA of 160˚.[81] Lotus effect is an ideal model for superhydrophobic self-cleaning derived from lotus plant characteristics. The other key components influenced high performance of lotus superhydrophobic surfaces are as follows;[82]

i. the surface's epidermal structures designated with micro-roughness;
ii. the formation of nanoscopic epicuticular wax crystals along leave surfaces; and
iii. superhydrophobic stability under moisture condensation conditions (i.e., no significant loss of the property of water repellency).

The hydrophobic surface of lotus leaves (Figure 3 (a-c)) is epicuticular waxy crystalloid, leading to form low surface free energy, micro-/nano-roughness, and superhydrophobicity of surfaces.[80-83] According to the effectiveness of lotus-simulating micro-/nano-surface roughness, the first artificial superhydrophobic surface was successfully fabricated in 1990s.[20]

Several on-surface methodologies such as etching, lithography, biomimetic and stamping were applied to fabricate superhydrophobic, dynamic nano-surface tectonics. A facile method of dispersing nanoparticles (NPs) in a hydrophobic polymer matrix leads to fabricate hydrophobic polymer/NP composite surface coatings.[23] The increase in the solid–liquid interface can increase both the surface roughness and its hydrophobicity by air trapping within grooves and interfaces. In addition, the rough surface is amplifying the superhydrophobicity because the air is superhydrophobic feature with WCA of 180°.[84] Micro-/nano- structure and the low surface free energy (SFE) along anisotropic surface heterogeneity of composite building blocks are thus responsible for surface superhydrophobicity.[85] Superhydrophobic composite surfaces are extensively used in engineering membrane, coating, self-clean system, and molecular dynamic applications.[1]

Figure 3

4.2. Rice- and butterfly wings-simulating surfaces in antifouling design

Not only lotus leaves' surface has water non-wettability characteristics, but also other plant leaves (e.g. rice leaf) and insect wings (e.g. butterfly) show similar "lotus effect" features.[86] As a result of entrapping air voids on the surface grooves of the micro/nanostructures, these leaves showed superhydrophobicity. Rice leaves (Figure 3 (d and e)) showed anisotropic texturing and minimum contact angle hysteresis (i.e., CAH << 10°) with micro-roughness along the leaf and various micro- and nano- surface pins. The surface core of the rice leaf has waxy nano-bumps with longitudinal grooves and transverse sinusoidal structure, but its top-ends have eggbeater structures with four cohered hairs. These ridge terminals have hydrophilic features for enhancing air-retaining ability underwater sources, which provide superhydrophobicity.[87] In turn, the butterfly's wings (Figure 3 (f and g)) possess superhydrophobicity as a result of the micro- and nanostructured surface. The microgrooves on butterfly wings afford a rough surface with superhydrophobic characters and low adhesion features. The confinement in the anisotropic-flow directions along leaf or wing orientations, vacancies, rigidness and interfaces provided self-cleaning surfaces of the rice leaves and butterfly wings.[88]

Together, such natural superhydrophobic surfaces incentivize the design of superhydrophobic self-cleaning surfaces and antifouling features, mimicking these natural surfaces.[80, 89]

Other surfaces like the legs of a water strider possess superhydrophobic surfaces (Figure 3 (h and i)).[90] The leg surface exhibits oriented microsetae that covered with needle morphology and grooved nanostructures. These surface features produce microroughness and water-repellent structure.[91] The legs' superhydrophobicity (Contact angle of 167˚) is caused by trapping the air in the surface nano-grooves. This feature permits the survival of water striders on the water surface.[80,92] Taro leaves have micro/nano-texturing with WCA of 159° as well as a sliding angle of <3°.[93]

4.3. Shark skin effect as self-cleaning, antifouling surfaces

High performance antifouling, self-cleaning, and low drag features were reported for fast-swimming shark skin. The low drag was caused by dermal denticles and the micro-structured riblets, which inhibited fouling attachments more than other marine organisms. A comparable study showed that the humpback whale skin (Figure 3j) was covered with barnacles; while the skin of the mako shark remained clean (Figure 3k).[94] The mako shark skin denticles could also enhance water flow rate, reduce surface drag, and inhibit fouling attachments. The shortfin mako was used for studying the self-cleaning feature. The surface of isurus oxyrinchus mako shark (one of the fastest sharks worldwide) is covered with tiny, flexible, teeth-like scale dermal structure, longitudinal grooves and ribbed structures, enabling fouling antiadhesion. In the shark skin structure, lifting and pinning could decrease the shear stress and cross-stream motion of fluids.

The shark skin is wrapped with fine tooth-shaped dermal surfaces that have longitudinal grooves with ribbed structures, as reported by Bechert et al.[95] Such grooves decrease the whirlpools formed on the ultrasmooth shark skin, leading to afford superhydrophobicity. In this regard, silicone-based shark skin-like nanostructured surface exhibited high fouling-prevention against different micro-organisms.[96] For an advanced market technology, commercial and powerful products were developed on the inspiration base of shark-skin surfaces, such as Speedo Fastskin fabric racing swimsuit.[97] Based on shark skin inspiration, further fouling-prevention surfaces were designated the pattern of Sharklet™ micro-textured film with a riblet morphology, which could remove fouling organisms.

4.4. Fouling release and self-cleaning coatings

The prevention of fouling attachments and reduction of fouling-coating adhesion strength is based on the controlled mechanisms that featured the FR surfaces. Non-toxic FR nanocomposites are a new trend toward robust eco-friendly self-cleaning coatings for vessel bottoms and shipping industry. These FR surfaces exhibit several merits such as non-toxicity and non-leaching (Figure 4). These features provide low friction and ultra-smooth surface of the ship hull, extreme molecular mobility, reduced free energy, micro/nano-roughness, tin-free, long-lasting durability.[98,99] The FR characteristics lead to reduce the fuel consumption and maintenance costs with increasing the ship speed and reducing the cargo days.[100]

The silicone paints exhibit inherently excellent FR features, but the addition of inorganic nano-additives has become inevitable for boosting the mechanical and FR characteristics of a wide-range of silicone paints.[99,101] Inorganic–organic surfaces can improve the superhydrophobic and antifouling abilities and reduce the free energy of the surface (Figure 4).[102] PDMS coatings were enriched with various nanofillers (including Fe_3O_4 nanospheres, TiO_2@SiO_2 core-shell, Cu_2O nanocubes, Al_2O_3 nanorods). These nano-structures are considered as efficient superhydrophobic FR nanocomposite surfaces.[1,18,19,103]

Figure 4

Graphene materials are of unpanelled properties as biocompatibility, economics, corrosion resistance and eco-friendly security, for potential applications.[103, 104] Silicone/graphene-based nanocomposite coatings can offer FR self-cleaning systems with mechanical durability and cost-savings.[105] GO/metal oxide hybrid represented a reinforcing FR nanofillers. These hybrid nanofillers can provide superhydrophobic and micro/nano-rough self-cleaning surface. All of these features are the key component characteristics of successful antifouling coatings.[106-108]

Self-cleaning materials included superhydrophobic and superhydrophilic surfaces have criteria to clean their surfaces from dirt and water. For example, superhydrophilic surfaces with contact angles of <10° can be produced through photo-induced catalysts that boosted by solar light irradiation for impurities breakdown. The mechanistic self-cleaning of such superhydrophilic materials under photo-induced lights may consequently follow the steps of (i) breakdown the structure of the adsorbed toxicant species, (ii) reduced the contact-angle on surfaces, and then (iii) release/remove the pollutants from surfaces.[103,104] In turn, self-cleaning mechanics of superhydrophobic materials may occur through water drop rolling that enabled to form thin-slide films as protective layers, leading to enhance the early-stage adhesion of pollutants.[1,109] These superhydrophobic surfaces are highly water repellent, which can prevent fouling settlement and decay surface-fouling adhesion bonds.[110]

5. Polymer fouling release nanocomposites

To date, nano-surfaces coated with FR paints should have low drag resistance, non-toxicity, non-biocidal, tin-free, smooth, chemically durable high solid content. Along with that features, biocides should not be released into the sea, and surfaces are. Accordingly, these FR surface paints would maximize the vessel speed and minimize the fuel consumption. Moreover, these building-block FR paints may extend the fouling control for prolonged service life (≥ 5 years). With these effective FR coating, maintenance and repairing costs would be reduced.[111, 112]

Although FR coatings have been developed since 1970s, their commercial production was started in 1980s as a result of the great demand for speedy trading and naval ships. The FR coatings are widely used after moving to apply ban TBT-based antifouling coating. It was firstly applied on a full fast ferry in 1996, where the ferry exhibited higher speed than that one coated by a copper-based antifouling paint.[113] Flouro and silicon polymers were used to synthesis FR coating under workability of reduced friction and low fouling-surface adhesion forces. In this regard, the fouling strains cannot be settled on the surface.

5.1. Homopolymer reinforced with nanofillers

The production of these hybrid nanocomposite coatings using inexpensive, environmentally friendly, and scalable methods has great influences in the large-scale synthesis and application of hybrid materials. With extensive investigations on functional hybrid nanocomposites, innovative advanced materials used in high doses have been developed.[114] Proposed nanostructured polymeric coatings are promising materials because they can control the release of metal species and exhibit easily modifiable biostatic properties. Interestingly, NPs hybrid polymer matrices have been widely explored because of their various physical and chemical properties, in which lead to enhanced stability, and film-forming ability.[115] Synthetic methods have been generally employed to avoid agglomeration. These methods included well-distribution of the nanomaterials through (i) ultrasonication, (ii) mechanical treatment (such as grinding), and (iii) surface-modified function groups of the nanomaterial surfaces.

Intra-particle interactions are difficult to break through conventional mixing because of their strong binding within formation of intra-NP interactions.[116] Thus, a well-defined dispersion technique should be developed to fabricate nanocomposite membranes. Polysiloxane resins (especially PDMS) are widely used to produce polymeric nanocomposites because of their high heat and UV resistance, hydrophobicity, low glass transition temperature (Tg), and antifouling properties. Many studies have focused on PDMS nanocomposite preparation. Development of different inorganic nanomaterials (including Al_2O_3, Fe_3O_4, TiO_2, Ag, and SiO_2, natural sepiolite, and MWCNT) would offer the formation of nanocomposites with unique physico-mechanical, -thermal, light-induced, and -electrical surface features, leading to control a wide range of potential applications.[117-120] For the fabrication of nanocomposite coating systems, dominating the size, type, and morphology of the nanofillers can enhance not only the antifouling properties but also the mechanical robustness. Insertion of <0.1wt.% of MWCNT in PDMS has been reported to enhance the FR behaviour against different organisms without changing the bulk mechanical features.[96,121] Also, using natural sepiolite ($Si_{12}O_{30}Mg_8(OH)_4(H_2O)_4{\cdot}8H_2O$) as nanofillers within vinyl terminated PDMS matrix enhanced modulus of elasticity of resultant hybrid composites. This high elasticity modulus of nanaocomposite was due to the large surface area associated with other surface interfaces and vacancies such as channels, micropores, fibrous nature, and the nanometric size (5–10 nm diameter).[96,121] This nanocomposite showed excellent hydrophobicity and antifouling performance toward definite fouling strains such as Ulva and zoospores. The dispersions of low-concentration MWCNT formed special antifouling features with no effect on coating robustness. The high CH–π interaction bondings with the methyl side chains of PDMS render the molecular mobility to be more facile.[122] On the other hand, single-wall CNTs were reported to be promising nanofillers to reinforce the PDMS-based superhydrophobic coating structures.[123,124] Controlling the nano-filling percentages is necessary to avoid agglomerations, cracking, and brittleness caused at high nanofiller concentrations.[125] Furthermore, silicone-based compounds are not leachant and hence environmentally controversial, although they provide high FR performance toward living organisms. Other essential parameters such as the increase in the molecular weight of PDMS is usually associated with low surface tension, leading to improve the superhydrophobicity and antifouling behaviour.[126]

5.1.1. Fluoro-polymer coatings

The fluoropolymers have non-porous, ultrasmooth, and low free energy surfaces. These fluoropolymers are promising resins for fouling release through physical anti-adhesion performance.[1] Also, these polymers have low Tg, which may reach to the room temperature, and hard and glassy backbone, leading to the feasible function as FR coating in very low thickness (~75 µm). However, these fluoropolymers exhibited disadvantages as follows;

i. low structural mobility because of the fluorine stiffness that hinder their rotation along the entire polymer backbone;[127] and
ii. the failure on the substrate-adhesive bond can be only induced by applying high critical stress, as these fluoropolymers yield higher bulk modulus than that of other elastomeric materials.[128]

These features indicated that the attached fouling strains on the coated surfaces cannot be easily eliminated from the surface.

5.1.2. Silicone-polymer coatings

PDMS-based FR surfaces are extensively utilized owing to their extremely smooth topology, low surface tension, and high elasticity modulus, and Tg, respectively. Based on their structurally-arranged molecular mobility, the PDMS surfaces inhibited the attachment of fouling functional units. Owing to their resemblance in the structure (R_2SiO) with that of ketones (R_2CO), silicone was used widely in FR coatings. The length is 1.64 Å for the siloxane backbone bond, while that of carbon-carbon bond is 1.53 Å. The long siloxane linkages in composite matrices can make the structural rotation more facile.[129] The PDMS showed a configuration of α-helix direction, which affords open structure, bond flexibility, and rotation through 180° with reduced rotational barrier. This polymer also exhibited the lowest Tg among all other polymers (~ −120 °C) and low free energy of the surface (~ 20-24 mJ/m^2).[130] Also, PDMS has torsional barrier, which allowed high flexibility and free rotation.[131] Minimum adhesion properties coincide with the lowest elastic modulus, indicating that the modulus of elasticity could also affect the silicone FR surfaces.

Industrial market for silicone has continuously expanded. The demands for silicones are high in several industries, especially FR self-cleaning coatings. The significant FR coatings of silicones were because of their unparalleled fouling inertness, hydrophobic character, and thermal and UV stability.[132] The international chemical industry has witnessed strict legislations for environmental protection, which urged the booming of silicone industry especially coating market.[134] Owing to the superior biological, physico-chemical and mechanical tendency, silicone coatings were utilized for various fields ranging from marine to space applications. [129-133] With respect to evaluations of the market, 17.2 billion US dollars were achieved by the silicone products in 2017, owing to their extra-ordinary applications.[132]

PDMS was extensively applied for self-cleaning because of its rough surface topology and hydrophobicity. PDMS-based shark-like nanocomposites prohibit micro-organism attachments onto surfaces.[133,134] As a promising field for sustainable material applications, design of silicone-based micro-/nano-rough surfaces can be applied for fouling-prevention applications.[122]

PDMS-based films offer coatings with non-toxicity and stability. The fabrication of PDMS-based films is a successful way to prevent fouling through physical fouling anti-adhesion and self-cleaning mechanism. As a FR coating matrix, silicones are more effective than fluoropolymers. The stiff fluorine atoms along their structures make biofouling attachments, which they cannot be easily released.[135] However, a major drawback of the PDMS homopolymers is the poor mechanical features that can be achieved even at extremely-high Mw (500,000 g/mol).[136] This drawback can be overcome by insertion of inorganic nanofillers in the polymeric matrix to produce nanocomposites with improved superhydrophobicity and anti-biofouling.[137]

Selected nanomaterials are designed in nanocomposite building blocks according to their high surface area, fouling resistance, cost-effectiveness, and chemical and corrosion resistance. Our research group was successfully prepared antifouling systems based on silicone-filled spherical Ag NPs, and PDMS/Cu_2O nanocube composites. Efficient FR techniques were fabricated through the developed nanocomposites of PDMS-filled with hybrid nanofillers (see Figure 1). The function between self-cleaning of PDMS coating surface and its durability is controlled by the morphological shape and size, and amount percentage of nanofiller insertion. Inorganic nanofillers are one of the promising solutions for superior nanocomposite coatings. Various nanomaterials such as Al_2O_3 nanorods, TiO_2 nanospheres, Ag@SiO_2 core-shell, GO/Al_2O_3 hybrid, and hybrid graphene-materials have been introduced to modify FR coatings based on reinforcing the physical, chemical, and mechanical performance.[1,131,138]

Hybrid nanofillers, such as core-shell structure materials, were also used to improve the FR and self-cleaning effect of surfaces. Superhydrophobic coatings based on PDMS and TiO_2/SiO_2 hybrid particles were fabricated for photocatalytic and self-cleaning performance.[139,140] Also, innovative silicone-based FR nanocoating was fabricated through in-situ method using ZnO@SiO_2 fillers with small concentration. These methodological routes are represented the environmentally friendly and inexpensive antifouling solutions.[108]

Our efforts were widely extended to offer ultrahydrophobic nanocoatings based on organosilane filled with SiO_2 nano-archetcutures.[141] Also, an ex-situ silicone-enriched SiC NW composite was introduced as FR coatings. This building-blocks system showed surfaces with micro-/nano-rough topology, minimum free energy, and superhydrophobicity, **see Figure 5**.[9] High molecular weight PDMS resin with vinyl ends was facilely prepared through chain-growth polymerization and cured by a mechanism of hydrosilation. The outcomes confirmed that excellent distribution of SiC NW fillers (0.5 wt.%) can lead to maximum WCA (153°) and minimum SFE (11.25 mN/m). The heterogeneous surface roughness was caused fouling release. A real-application in the field test was performed in natural seawater of tropical area for 3 months. The obtained results exhibited the high FR properties.

Significantly, an evidence of the effective ex-situ design for nanocomposite fabrication based of PDMS/β-MnO_2 nanorod (NR) building blocks was approved.[141] β–MnO_2 nanorods with 20-30 nm wide, 0.5-1 µm long single-crystals, and wurtzite structure preferentially grown in [100] direction were prepared via a hydrothermal reaction followed by calcination. Excellent distributed nanorods in the silicone matrix exhibited the preferable self-cleaning with WCA of 158° and SFE of 12.65 mN/m, which provided FR performance. The uniform packed array of β-MnO_2 nanorod oriented with

[100] crystal plane causes micro/nano hierarchical roughness and superhydrophobicity. Selected micro-foulants including gram-positive and gram-negative bacteria, yeast, and fungi were used for biological and antifouling assessments in laboratory up to one month. Well-distribution of nanofillers enabled a reduction of biodegradability and enhancement of FR features. These nano-tectonic confinement composites enabled air-entrapping along interfacial surface grooves, and along well-ordered configuration in multiple exposed direction domains (i.e., edges, apex, and faces of NRs), leading to the formation of promising FR and self-cleaning coating, as shown in **Figure 6**.

Figures 5
Figures 6

5.2. Silicone-based polymer (PDMS) enriched with carbonaceous nanofillers

Carbonaceous nanofillers, especially carbon nanotubes (CNTs) and graphenic materials can develop superhydrophobic surfaces. Sun et al. [142] reported that the incorporation of CNTs in the PDMS resin improved the efficacy against biofouling. Graphene, graphene oxide (GO), reduced GO (rGO), and graphitic carbon nitride (g-C_3N_4) are represented as graphene-related materials.[30]. These material-types exhibit ultrahigh mechanical stiffness, high conductivity, extra-ordinary electronic transportation, and ultrahigh thermal conductivity; as a result of their two-dimensional structures. These graphene-related materials can provide efficient nanofillers for FR coatings. These carbon-based nanocomposites are commonly utilized nanomaterial in various applications such as biotechnology, green energy and environmental chemistry.[143]

Graphene is the strongest material ever tested. An antifouling coating of graphene–silicone rubber composite membranes was produced as an eco-friendly material.[144] Zhang et al.[145] reported the fabrication of water-repellent nanocoating filled with graphene materials with high robustness and self-cleaning. However, there is a trade-off between the coating's FR properties and durability after immersing under seawater for long period. Also, these types of graphene nanofillers showed merits/de-merits in their composite building blocks as follows;

i. the large surface energy of graphene nanofiller materials may cause agglomeration and prevent the uniform distribution within the polymeric matrix. This heterogonous building block definitely deteriorates the coating durability and its flexibility,
ii. agglomerated GO nanofillers in the polymeric matrix can be prevented through well-distribution and using suitable nanofiller percentages, and
iii. decoration of graphene materials with other nanoparticles such as metal and/or metal oxide nanomaterials can enhance the extent of nanofiller dispersion in the polymeric matrix.

In this regard, we developed a silicone-based nano-surface that enriched by well-dispersed GO-alumina mixture (Figure 7). [146] γ–Al_2O_3 NRs of 150 nm in length and 20 nm in diameter were fastened between GO nanosheets through a two-phase method and conformably coated with silicone layers. A ternary nanocomposite series of elastomeric silicone/GO-Al_2O_3 hybrid coatings was newly developed via a solution casting method and applied for FR coatings of ship hulls. Well-dispersed GO-γ-Al_2O_3 hybrid nanofillers up to 1 wt. % would increase the WCA to 151°, decrease the SFE to 13.25 mN/m, and provide micro-nano roughness. High thermal stability was caused by well-dispersion of nanofillers. The mechanistic insertion of nanofillers into plymer nanocomposite channels leads to form an H-bonding interaction that restricted polymer chain mobility. Our building blocks of nanocomposites showed ultrahydrophobic fouling-prevention nanocoating for vessel hull.[146]

Figure 9

5.3. Copolymer brushes nanocomposite with nanofillers

Improvement of both FR coating and mechanical robustness of the marine surfaces is recently at the research level.[147] Silicone-block copolymer is a major motivation to enhance the strength and mechanical robustness of organic polymers. Accordingly, the PDMS surfaces featured self-cleaning for antifouling application in the marine environment. However, some drawbacks of using silicone FR coatings were listed on the base of the trade-off between antifouling performance and mechanical features. The preferable composite surfaces revealed renewable self-cleaning features at higher mechanical properties and long-term performance.[148] Some micro-organisms such as diatoms have the ability to adhere a hydrophobic surface and cause surface deterioration. It is necessary to rational control the relationship between the mechanical features and FR performance during the fabrication of nanocomposites.[149] The rational fabrication of nanocomposites can reduce the friction resistance, increase vessel speed, and lengthen the dry-docking intervals.

With respect to the stability in seawater, silicone RTV11-based surfaces showed coating with 0.02 wt %/ mass loss per week because of the removal molecular-weight materials (including linear and cyclic unites) and depolymerization.[150] However, vinyl terminated PDMS (Sylgard 184) is fairly stable in the seawater. The reduction of the WCA of fluoropolymers and PDMS based coatings was reported after immersion in seawater.[151,152] The key clues may be due to the thermodynamic rearrangement of polymeric chains, which carried out through the surface polarity of the interface between matrix/water layers.

An interaction between secreted bio-adhesives and antifouling coating may be caused by the enhanced polarity of FR coatings, which enable fouling attachments and loss of FR characteristics. However, incorporation of silicone oil with low viscosity can delay the changes in the surface chemistry of the coating after immersing in seawater.[153] Also, FR films suffer from poor adhesion to the epoxy anticorrosive primer. To overcome this adhesive problem, the addition of tie-coat may represent a necessary step for providing high cohesion between epoxy primer and silicone layer. The PDMS-based FR coatings have low elastic modulus; this soft structure offers week mechanical features. Thus, the resultant coating is susceptible tearing, cutting, and puncturing. Modifying homo-silicone polymer with NPs may affect the tensile modulus and produce stiff surface with low FR properties.[154-156] The silicon-polymer-filled NPs building blocks can reduce the dry-docking intervals of the ship hull coating and increase the shipping costs.[157-161] Using silicone-based block copolymer composites can provide high mechanical features, durability, robustness, and renewable self-cleaning features. The copolymers can be applied directly on the epoxy tie-coat, leading to cost-effective antifouling solution. The high durability and renewable FR self-cleaning features can cause high speed, elongation of the dry-docking intervals, and reduction of the shipping costs.

5.3.1. Copolymer brush for FR coating applications

There is a trade-off between FR and durability of silicone coatings. In order to develop a durable coating surface for FR and self-cleaning application, silicone copolymers were synthesized to hybrid PDMS with other polymers or segments such as polyurethane, epoxy, methyl methacrylate and fluorine units.[162]

Block copolymers fabricated from poly(methyl methacrylate) and PDMS would enhance the mechanical surfaces and antifouling advantages of these two components. Fabrication of multi-components via new method, namely electro-spinning, would facilitate the compatibility between the two polymers and offer many unique FR properties. This method will endow their copolymers to fabricate micro-phase structures.

Modifying PDMS with polyurea can provide high mechanical features, FR properties, and corrosion protection. These characteristics are induced by the interaction between the isocyanate groups with the residual hydroxyl groups of the epoxy primer's surface (Figure 8).[163] A copolymer of polyurea with α,ω-aminopropyl terminated PDMS as soft segments and 1,6-hexanediamine as a hard segment was developed via a poly-condensation reaction. The produced surface revealed hydrophobic with WCA > 90° and SFE of 25–29 $mJ{\cdot}m^{-2}$. Because of its lower toxicity, isophorone diisocyanate (IPDI) is more preferable than that of 4,4'-diphenylmethane diisocyanate (MDI) or toluene-2,4-diisocyanate. IPDI can also yield more flexible polymer chain, which is favourable to reduce the polymer modulus. This PDMS/polyurea composite can provide high substrate-coating adhesion forces.[164] PDMS-polyurea hybrid surface exhibits high toughness, mechanical features, low free energy, micro-/nano-roughness, and FR features.

Figure 7
Figure 8

5.3.2. Fluorinated-silicone coatings and controlled-synthesis of nanofillers

In order to achieve high FR features, low surface free energy, and durability, fluorinated-silicone coatings were developed to enhance polymer merits. Low free energy, non-porosity, and non-stick characteristics are introduced by fluoropolymers. However, these polymers suffered from restricted mobile structure that caused by fluorine stiffness. On the other hand, the reduction of elastic modulus and free energy, and the elevation of water-repellency and high fouling-prevention were introduced by silicone-dependant FR nano-surfaces. Fluoroalkylsilanes were used not only as a matrix but also as a surfactant to reduce the surface free energy.

Another avenue to produce fluorinated-silicone coating is to use fluorinated-CNTs as nanofiller to enrich PDMS. Nanofiller insertion to this building blocks may reduce the surface tension by fluorine atoms, leading to high FR, and durability.[165] Controlled synthesis of GO decorated with one-dimensional (1D) nanomaterials (β-MnO_2 and γ-Al_2O_3 nanorods) represent effective antifouling filler materials.[26]

Furthermore, the anchoring of rGO into cubic Cu_2O particles represented a promising nanofiller for FR and self-cleaning application.[26,166] The GO is usually prepared through a modified Hummer method and followed by reduction process to produce rGO. It is also reported that the Cu_2O nanocubes were prepared and controlled through a wet chemical technique at RT without using any surfactants or templates, which are usually toxic and difficult to wash.[116] Two-phase method can be used to prepare nanocomposite of rGO/Cu_2O hybrid. High antibacterial and antibiofilm activities of rGO/Cu_2O hybrid were explained on the basis of the wrapping effect toward the bacterial strains, in addition to the ability of the hybrid to change the bacterial cell morphology and kill them.[167] Such innovative building blocks lead to fabricate self-cleaning, and ultrahydrophobic polymer nanostructure composites for maritime navigation. The designed nanocomposites can yield eco-friendly marine ecosystem.

5.3.3. Design of micro-/nano-rough antifouling structure surfaces

The superhydrophobic self-cleaning designs based on nanostructured, micro structured, and micro/nano-hierarchically-oriented surface roughness are essential parameters for increasing the superhydrophobicity of the coating surface than the flat solid surface (Figure 9). These nanocomposites can offer an excellent fouling-prevention form adhesion by physical anti-adhesion mechanism.[168] Following Cassie–Baxter approach, the dense layer of the nanocomposite with improved rough surface topology enabled air entrapping within the interstices of the surface grooves. This surface behaviour prevents water sliding inside these holes, and produces water-repellency through amplifying water-repellency, when the air contact angle is 180˚. As a result, the water is unable to penetrate the nano-grooves, leading to cause self-cleaning system. Surface roughness produced air pockets between the liquid drop and solid surface, which is related to the chemical heterogeneous structure of the nanocomposite. High micro-/nano-structure designated over a rough surface can prevent the transition from Cassie-Baxter state to Wenzel state. This nano-/micro-surface can also lead to increased non-wettability, stable self-cleaning, and enhanced FR features. [165] As a result, PDMS-based block copolymers incorporated with hybrid nanofillers of graphene/1D-metal oxides are promising to develop robust self-cleaning and FR coatings. In this regard, the micro-/nano-rough antifouling surface with low free energy can inhibit coating-fouling adhesion bonds.

Figure 9

5.3.4. Key controls of nanoscale filler tectonics in antifouling coatings

Understanding the key functions of nanoscale filler tectonics in terms of its surfaces, atomic-scale crystal structures, architectures, and textural parameters can develop cutting-edge environment and super-smart antifouling coatings. In this section, we provide evidence of the effect of nanoscale filler tectonics to fabricate structurally folded nanocomposite building-blocks, which create outstanding superhydrophobicity, self-cleaning surfaces and potential antifouling coatings. Different nanoscale fillers such as metal oxides, natural sepiolite, and carbon-related materials were used to fabricate PDMS-based FR tectonic surfaces. For example, dispersion of MWCNT fillers (0.1 wt.%) within PDMS matrix can improve fouling-prevention, and coating functionality and durability.[169]

Natural sepiolite $Si_{12}O_{30}Mg_8(OH)_4(H_2O)_4{\cdot}8H_2O$ is incorporated in PDMS for improving the nanoscale surface fouling-prohibition at stable modulus of elasticity.[170] The sepiolite fillers can form micro-channels, which can entrap air and cause hydrophobicity. PDMS with its siloxane bonding affinity allows the well-defined distribution of nanofillers through covalent bonding, leading to form nanocomposite surfaces with fouling-prevention of attachments. It was also reported that dispersion of low percentage of MWCNTs (i.e., 0.05%) in the silicone matrix can enhance the coating non-wettability and maximize fouling-prevention by 50%.[171] The CH_3 terminals of PDMS offer surface mobile structure of the polymer. Controlling the structural types, composition, hierarchy, particle size, and shape morphology of nanoscale filler tectonics can provide superhydrophobic surface structures for self-cleaning and FR applications.[172] Many methods such as sol-gel, electrochemical deposition, plasma treatment were used to develop these surfaces during the fabrication of structurally folded nanocomposite building blocks.[173] Water-repellant nanoscale surfaces can be optimized by dispersion of different nanofiller composition and their concentrations including metal oxides, noble metals, graphene-based materials for fouling-prevention. Nanofiller concentrations in the polymeric matrix can also dominate the surfaces micro/nano-roughness, and anisotropic heterogeneity through dominating the structure-folded properties, atomic-scale arrangements, hierarchal models, and configurations along the entire nanocomposite building blocks. A micro/nano-roughened surface was developed through dispersion ZnO nanoscale filters in the entire surface of polymeric matrices.[174] A fouling-inhibition nanocoating was synthesized through dispersion of nano-magnetite materials in the PDMS matrix-supported aminopropyltriethoxysilane to yield ultrahydrophobic surfaces with a WCA of 158.3°.[175]

Towards the control of nano-tectonic confinement composite building blocks in fabrication of self-cleaning system, superhydrophobic composite of silicone/micro- $CaCO_3$/nano-silica was fabricated.[176] Also, a self-cleaning surface of organosilane filled with nanoscale SiO_2 was also reported by Li et al.[174] A fouling-repellant, superhydrophobic composite of polysiloxane filled with alumina nanorods (NRs) was fabricated through in situ procedure for fouling-prevention.[24] Confinement of composite building blocks was not only depended on the nanofiller structures, types, or compositions but also on the dispersion and concentration of nanofillers, which played a key broadening role in the fabrication of highest self-cleaning surfaces, and water and fouling-repellancy. Furthermore, an effective FR was synthesized using silicone/magnetite nanosphere building blocks that significantly offer composite surfaces with WCA of 153°, reduced free energy (13.91 mN/m), and micro-roughness.[137]

A PDMS-based fouling-prevention composite coating filled with core/shell nanospheres of Ag@SiO_2 provide sustainable surface coatings that have been attained in the seawater for 3 months (Figure 10).[177] A confined synthesis of Ag@SiO_2 NPs using solvothermal and Stöber methods leads to control Ag@SiO_2 with 60 nm diameter size, crystal structures, and direction along actively-exposed {111}-plane surfaces. Ag@SiO_2 core–shell nanofillers were inserted in the silicone composite surface via an ex-situ method. A simple hydrosilation curing mechanism was used to cure the silicone nanocomposite coating. The key development is the confinement alignment of filler NPs along the polymeric matrices, leading to improve the fouling-antiadhesion and develop nanoscale surface with WCA of 156°. This surface also exhibited low free energy (11.15 mN/m) and non-toxicity. [177] The CA hysteresis and the difference between the advancing and the receding CAs were assessed from the dynamic CA measurements. The lowest CA hysteresis (6°) and the highest WCA were achieved for well-dispersed nanofillers. The dispersion control was led to highest self-cleaning and FR features. In addition, the cell viability measurements were carried out by using different microorganisms. The cell viability is reflected the decrease of the microorganisms' number and increase of the bacterial growth inhibition that can be occurred with well-dispersion of nanofillers. In this regard, a wide range of confinement synthesis methods were used to fabricate efficient composites such as PDMS/SiO_2 and silicone/polystyrene/ SiO_2 building blocks with minimum free energy, superhydrophobicity, and self-cleaing characteristics.[178,179]

An in situ terminology was followed to prepare a FR coating of silicone-enriched ZnO NR composite (Figure 11), which is an eco-friendly and inexpensive marine coating solution.[178-182] A combination of wet-chemical

and hydrothermal methods was used to prepare ZnO NRs with 30–40 nm width and 0.5–1 μm length and wurtzite structure grown in (0001) direction. The most favourable FR properties with maximum WCA (158°) and minimum free energy (11.25 mN/m) were shown with addition of 0.5 wt. % NRs, leading to an excellent distribution of NRs onto surfaces. Stability of the WCAs of the coatings was evident by submerging the samples (for 10 days) in solutions and at various pH values. The produced nanocomposites exhibited high stability against different pH solution. A field trial was performed onto the virgin PDMS and well-dispersed nanocomposite surfaces. In practical sets, both materials were immersed (for 6 months) in marine water of a tropical region. The obtained results indicated the higher FR performance of the nanocomposite than that of virgin silicone surface.

Figure 10

Figure 11

5.3.5. Graphene-hybrid nanofillers and their synergetic effects

Graphene nanofiller distribution within the host polymer matrices represents a crucial parameter in polymer nanocomposite fabrication.[183] Because of its oxygen-rich functionality, GO can be distributed in water (or solvent) to single sheets. The features of graphene composites are based on graphene-host matrix and its interfacial bonding.[184] The physico-mechanical characteristics of GO structures depended on the polymer-GO hydrogen bonding interaction.

Grafting and chemical functionality can greatly enhance polymer-GO compatibility. It is difficult to disperse GO nanosheet in a hydrophobic matrix because of its polarity. Attempts were carried out for dispersing GO sheets in apolar organic solvent. GO layers are aggregated by the action of the oxygenated surface units. Organic functionality of GO surface can improve its compatibility with a hydrophobic polymer. Ethyl isocyanate was used to functionalize GO through opening the surface epoxy ring and provide dispersed GO in DMF solvent.[185] A poor distribution of graphene-materials in the polymer produces a nanocomposite with weak hydrophobic and mechanical properties. The weak interactions of polymeric-matrix with graphene results in reduced coating-substrate adhesion and elasticity. The chemical modification of graphene nanosheets is difficult because of low surface functionality. The hydrophobicity of graphene yields agglomerated sheets in an aqueous solution as a result of π–π restacking effect of graphene layers.[186] Grafting of graphene into polymeric-matrix aims to introduce graphene surface functionality and to increase the polymer hydrophobicity and compatibility in various solvents.

Functional graphene-nanocomposite surfaces represent a promising application field to develop superhydrophobic surfaces.[187] Graphene based nano-materials were applied for superhydrophobic membranes for preventing water penetration.[188] Outstanding electro-chemical and oxygen transmission are characterized the graphene based superhydrophobic networks. Several graphene-based nanocomposites are employed as electrical sensor actuators, and green energy applications.[189]

Graphene based superhydrophobic coating is promising candidate in many functions. Electrochemically exfoliated graphene and PDMS lead to form superhydrophobic coating surfaces. Self-cleaning, antifouling and anti-corrosive characteristics are promising achievements, when superhydrophobic paints were applied. Such surface superhydrophobicity showed ultra-strong coating with high water and chemical resistance. Indeed, graphene-based superhydrophobic surfaces were extensively applied as self-cleaning and fouling release (FR) coatings. Superhydrophobic nanocomposites with high WCA > 150°, low CAH <5°, micro-nano roughness and reduced surface SFE are promising surfaces for eco-friendly antifouling applications.[190] Graphene-filled elastomeric PDMS nanocomposite films offer excellent physico-mechanical and surface properties. Advances of nanocomposite paints based on graphene are growing rapidly to develop superhydrophobic self-cleaning materials with high antifouling performance. Graphene-based silicone compounds exhibit superior antifouling and mechanical features.[191] A graphene-based PDMS nanocomposite was developed as a coating material for surface self-cleaning and robustness (Figure 12).[192] The hybrid nanocomposite was fabricated by mixing PDMS, crushed GO, TiO_2 NPs and diatomaceous earth to yield surfaces with WCA of 172°, durability and corrosion protection with inhibition capacity of 96.7%. The coatings were applied by air-spraying method. The results indicated the development of self-cleaning and superhydrophobic surface. When applied on a PDMS adhesive substrate, the coatings were able to retain their superhydrophobic and self-cleaning properties after performing a tough mechanical damage by abrasion and scratching. Tafel analysis and potentiodynamic polarization studies confirmed the excellent corrosion-resistant properties with 96.78% inhibition efficiency.

Figure 12

A vacuum filtration technique was used to support a membrane of cellulose acetate with rGO/g-C_3N_4 hybrids.[193] The prepared microfiltration membrane composite exhibited superb photocatalytic and self-cleaning features, leading to degrade organic pollutants and eliminate bacteria. However, this surface modification was unstable and the nanocomposite did not provide filtration for a long-time due to the low membrane-substrate adhesion. A facile stable nanocomposite alternative was synthesized through blending method.[194]

Graphene nanomaterial leads to a dramatic change in the non-wettability, attributing to the effectiveness of surface roughness and chemistry of graphene sheets. Graphene sheets with superhydrophilic characters can be produced by sonication in water, while superhydrophobic character can be produced by ultra-sonication in acetone. The roughness parameter greatly influenced the surface superhydrophobicity. Hydrophilic graphene sheets were obtained by ultrasonication in water and applied in hydrophilic self-cleaning coating. However, hydrophobic graphene sheets were obtained through ultrasonication of graphene in acetone and greatly applied to enhance the surface self-cleaning and superhydrophobicity. Controlling the relative proportion of water or acetone is effective to yield superhydrophilic or superhydrophobic coating. WCA of graphenic-nanocomposite film is changed from hydrophobicity to hydrophilicity by dominating acetone/water ratio. This method is represented as an easy technique to fabricate non-wettable surface features. Graphite is oxidized to graphite oxide, which is subjected to rapid reduction and expansion exfoliation of sulfuric acid intercalated graphite oxide at 100 °C and in ambient atmosphere. The resultant sheets of graphene was fabricated as shown in Figure 13A.[195] The intensive heat may decompose the carbonyl groups bonding on the sheet edge. This process has the advantages of reductant free, easy operation, low-energy and environmentally friendly.

Together, graphene nanocomposites are introduced as eminent nanofillers for various applications as follows:

(i) efficient photocatalyst to hinder recombining the photo-holes,
(ii) formation of 2D structured forms with extremely large area to the surface volume, and
(iii) low energy band gap, robust and highly conductive materials.

Anchored graphene materials can lead to fabrication of outstanding surface materials with self-cleaning characters, and superhydrophobic and photocatalytic features. An inexpensive film of rGO/ZnO nanocomposite was fabricated for photocatalytic self-cleaning applications (Figure 13B).[196] These nanocomposites are photoinduced superhydrophilicity that can be enhanced with increasing the rGO/ZnO ratio. A high photocatalytic activity of the nanocomposite film is observed in the photodegradation of methyl blue in water after exposure to the sunlight irradiation. When rGO/ZnO NPs are exposed to the solar light, electrons and holes (generated carriers) are produced at energy band gap (E_{bg}). The photo-generated electrons (e^-) transfer from the valence band to the conduction band, while the holes (h^+) remain in the valence band. The e^- in the conduction band can reduce oxygen to superoxide anion radicals, while the strong oxidizing capability of h^+ can oxidize water to produce a hydroxyl radical. As a consequence, this radical can remove adsorbed organic pollutants and fouling organisms and easily self-clean nanocomposite surfaces. The dirt can also be destroyed by solar light to disintegrated parts and finally to CO_2 and H_2O. The utilization of graphene related composite materials for robust FR coatings is effective trend for eco-friendly smart photo-induced FR nano-paints.

Figure 13

6. Ternary and quaternary superhydrophobic fouling release nanocomposites

Block copolymers fabricated from the combination of poly(methyl methacrylate) and PDMS were enhanced the mechanical surface and antifouling advantages of these two components (Figure 14). Controlling the PMMA concentration, PDMS/PMMA mass ratio, and main parameters of electrospinning process (voltage and injection rate) is inevitable to obtain superhydrophobic surface with high WCA. It was reported that a high WCA of 163° could be achieved on the polymeric surface fabricated by electrospinning solution containing PDMS: PMMA: tetrahydrofuran (THF): N,N-dimethylformamide (DMF) (mass ratio 1: 1: 8.88: 9.48) under applied voltage of 11 kV and injection rate of 0.1 mm/min.[197]

Figure 14

PDMS/PMMA robust coating can withstand sand impact abrasion, water drop impact, and immersion in strong acid and alkali solutions. It has a homogeneous-plastic material and excellent salt rejection efficiency. Insertion of GO hybrid nanofiller in the PDMS/PMMA copolymer can provide higher WCA, surface micro/nano-roughness, lower SFE, and higher mechanical robustness than that of virgin polymer. These nanocomposites are promising robust self-cleaning and FR coating surfaces.[198]

Silicone-epoxy composites were provided durable FR coating material with enhanced adhesion properties between the coating and substrate. Modified trends of fluorine-silicone based coatings represented promising FR surfaces. A new method introduced to facilitate the compatibility between the two polymers. The two components were found to endow their copolymers with micro-phase structures. Also, hybrid nanofillers lead to outstanding distribution in the polymeric matrix and improve the fouling prevention. Ternary and quaternary nanocomposite building blocks were successfully developed by modifing polymer (copolymer) and enriched (hybrid) nanofillers using different techniques, as mentioned in Table 2.[197-210] These nanocomposite building blocks can provide surface coatings in wide range functions as follows:

i. development of applicable and environmental-friendly fouling prevention nanocoating with self-cleaning feature for vessel hull,
ii. providing of economic and environmental effectiveness, longevity, and coating robustness for shipping industry,
iii. non-toxicity and long-term durability of coating systems,
iv. achievement of high distribution of the hybrid nanofillers in the copolymer matrix, which enhanced the fouling-prevention, coating roughness, and fouling-prevention,
v. understanding of key effects of functionalization, nanofiller concentrations, and structure functions, leading to improve the foul release surfaces and self-cleaning, and
vi. development of advanced biomimetic nanomaterials to satisfy the demand of betterment.

Table 2

As a result, the designed silicone-based block copolymers incorporated with hybrid graphene/1D-metal oxide nanofiller are promising to develop robust self-cleaning, and FR coatings. The resultant composite building blocks showed evidence of formation of micro-/nano-rough antifouling surfaces with low free energy, which can inhibit coating-fouling adhesion bonds.

6.1. Silicone-polyurethane composites

Modifying of the silicone matrix with polyurethane represents an attempt for improving the robustness of the FR coatings. The hybrid silicone-polyurethane effectively leads to surface self-cleaning, low free energy, good toughness, and mechanical robustness of modified coating layer. Also, the presence of isocyanate units provided an enhanced adhesion between the copolymer and the epoxy anticorrosion layer without the need for a tie coat, as reported elsewhere.[211,212] A polymer network is produced through the hybridization of PDMS and poly(urea) or poly(urethane-urea). The PDMS-polyurethane layer form curing hydroxyl-ended polyesters and silicones for FR coating application.[213] The preparation of crosslinked PDMS–polyurethane coated films was achieved, which used as modifiers for FR alternatives.[214] Another cross-linked PDMS-polyurethane was developed as a thick-coated film by Majumdar and Webster.[215] The film showed a phase separation 10% of PDMS and produced micro-topographical structure as a stable hydrophobic surface.[216] This soft-hard combination improved the phase hybridization of polymers with reduced surface free energy and strong adhesion forces with the epoxy primer.[217,218] This polymer hybridization produced robust FR superhydrophobic structures with controlled surface structures and improved physico-mechanical features.

6.2. Silicone-epoxy composites

As a modified resin, PDMS-epoxy copolymer represents outstanding FR coating with high surface durability. A flexible PDMS-polyurethane crosslinked with polyether diamine showed biphasic morphology with low free energy and tensile modulus. High adhesion forces were produced between the coating films on primer layer. A PDMS modified with epoxy resin achieved 0.58 MPa of pseudo barnacle cohesion forces by insertion of 30% of PDMS, leading to form fouling-prevention coatings.

On contrarily, these coatings showed a drawback of surface reconstruction and migration of epoxy units after immersing in marine water. Insertion of hybrid nanofillers is an essential to develop superhydrophobic self-cleaning surfaces with improved mechanical features, which withstand the surface reconstruction and migration of epoxy units after immersing in seawater. Another silicone-epoxy copolymer developed tough coating film under treatment of UV irradiation. This copolymer used a cycloaliphatic epoxy-functionalized PDMS offered surfaces with ~ 45 MPa tensile modulus, which is higher than that of homo-silicone FR coatings. This copolymer is harder and more thermoset than that of soft elastomeric coatings. The cycloaliphatic epoxy-functionalized PDMS surface coating exhibited minimum surface free energy of 15 mN/m, high WCA, and structural stability in water. This polymer is represented as FR coating material with surface self-cleaning features.

6.3. Combined fluorine-silicone based materials

Fluorinated silicone coating is another eco-friendly solution. A combination of both silicone and fluorine non-stick characteristics in diverse macromolecular architectures, such as siloxane-fluorinated (co)polymers provided FR coatings.[173] Although, FR based fluorine coatings have low surface tension, the stiff fluorine atoms hindered the mobility of molecular structure, and thus leads to the difficult elimination of attached organisms. The FR based silicone coatings were fabricated with low surface tension, low modules of elasticity and mobile molecular configuration, leading to excellent fouling repellency. As a result, the poor durability of silicon polymers usually limits their applications.[175]

As a curing agent or a polymer moiety, fluorine compounds can be used to modify PDMS to yield copolymer coating with low surface free energy, FR, and chemical stability in seawater.[178] Nevertheless, fluorinated silicone copolymer-based FR films were highly improved by nanofiller addition. Nanofillers containing fluoro moieties enhanced the FR and mechanical efficiency of silicon paints.[131,219] Carbon nanotubes (CNTs) are one type of nanofillers that used to fabricate a silicone composite. Modelling of fluorinated CNTs to modify PDMS is a fascinating strategy to improve the fouling-prevention and surface self-cleaning than that of un-fluorinated PDMS/MWCNT composite, as reported by Irani et al (Figure 15).[164,220,221] The fluorinated nanocomposite showed 67% reduction in the pseudo-barnacle adhesion.[221] Fluorinated CNTs are an efficient solution for FR antifouling surfaces, which provided both the PDMS self-cleaning features, low surface free energy of fluorine and mechanical properties.

The critical surface energy of the cured PDMS films did not change in presence of the pristine MWCNTs; however, the fluorinated MWCNTs are reduced the critical surface energy. Fluorinated MWCNTs in the coatings are more effective than that of pristine type in reducing the surface-marine fouling adhesion strength and provide FR nanocomposite coatings for the ship hulls.[196] Together, a challenge to develop a facile, applicable, highly stable, eco-friendly and economic nanocomposite models for marine FR self-cleaning of vessel hulls still remains.

Figure 15

6.4. Other nanocomposites

An antifouling ternary nanocomposite was developed by using UF matrix enriched with Ag/GO hybrids.[222] Also, an antifouling nanocomposite of PSF-GO/SiO_2 membrane was developed.[223] A water permeable nanocomposite of polyethersulfone (PES) membrane enriched with TiO_2/GO hybrids exhibited nano-filtration properties with antifouling behavior.[224] This nanocomposite was also used for desalination through developing membranes with reverse osmosis.[225] The hybridized ZnO/GO revealed high photocatalytic response.

The existence of functional (hydroxyl, epoxy and carboxyl) units on GO surface facilitates its chemical functionalization and nanocomposite formation. High antifouling performance was confirmed for PES enriched ZnO/GO hybrids compared with the bare PES surface. The reduced non-electrostatic interactions between the PES and hybrid fillers provided enhancement in the antifouling features and rejection of trace-organic compounds.[226] A hybrid inorganic nanocomposite of Cu_2O/rGO material was fabricated, as reported elsewhere.[227] Cu_2O nanofillers with 4 nm size have been dispersed within the coating of r-GO nanosheets to form a stable nanocomposite with an outstanding electro-catalytic performance. Such nanocomposite was employed as a cathodic catalyst inside the fuel cells for oxygen reduction.[228] Development of an advanced category of rGO enriched with metal oxides is promising terminology for fouling-prevention.

A non-classical crystallization of mesocrystals rGO/nanowire Cu_2O composite hybrids was developed via hydrothermal technique. The prepared mesoporous rGO/Cu_2O composite demonstrated higher sensitive properties toward NO_2 than that of single rGO nanosheets or Cu_2O wire systems. Thus, the developed nanocomposite was extensively applied as environmental sensors with ultra-sensitivity.[228]

A self-assembly and in situ photo-reduction technique was used to prepare rGO/ZnO composite. The fabricated composite was used for self-cleaning and elimination of water pollutants.[229] As a unique structural property, rGO/ZnO composite could exhibit well-dispersed and dense NPs on the graphene surface. The rGO/ZnO demonstrated a higher photocatalytic activity for degrading of rhodamine B dye (RhB) than the neat ZnO NPs under simulated sunlight irradiation. The recoverable adsorption feature and increased photocatalytic activity of this composite supports its practical applications in the FR coatings.

Photo-reduction and deposition-precipitation methods were used to fabricate a photocatalytic nanocomposite of GO/g-C_3N_4 supported with Ag-AgCl hybrids for environmental purification. The produced nanocomposite can degrade methyl orange and methylene blue in the visible region.[230] An antibacterial nanocomposite of GO/g-C_3N_4 hybrids was designed with photocatalytic properties via sonochemical technique at ambient temperature (Figure 16).[211] The introduction of GO is contributed to separate photo-generated electrons and prevented the electron−hole pairs of g-C_3N_4 from re-combination to generate more h^+, thus directly improving the bactericidal ability of GO/g-C_3N_4. The nanocomposite approved antibacterial efficiency against Escherichia coli and also a stable photocatalytic feature after using for four times and applied for water purification

Figure 16

Furthermore, sonochemical technique was used to fabricate a GO modified g-C_3N_4 nanocomposite to achieve effective photocatalysis through visible region for waste control. Research developments of fouling-resistant coating materials based on controlling the micro-/nano- structural designs are in a high level today.

7. Design of micro-/nano-structure and surface texturing design

Controlling the nanoscale structures presented a new technology for developing micro-/nano-roughness and superhydrophobic nano-coatings.[196,231] The increase in the solid–liquid interface enhanced both the surface roughness and its hydrophobicity by air trapping within the surface grooves and under the water droplet. Micro-/nano- structured surfaces and SFE are thus responsible for superhydrophobicity.

7.1. Modern superhydrophobic designs

Superhydrophobic surfaces are extensively used in engineering wide-range of composite building blocks with diverse features;

a. novel self-cleaning and fouling-prevention coatings based on silicone-containing copolymers filled with graphene/metal oxide nanocomposites, leading to improved FR and durability features,
b. these superhydrophobic surfaces displayed micro-/nano-scale roughness and self-cleaning, and mechanical durability due to the nanofiller enrichment,
c. suitably dispersed nanofillers in the polymeric nanocomposites at different loading concentrations would modify the physico-mechanical and self-cleaning behaviour,
d. micro-/nano-roughness, well-distribution of nanofillers, slippery surface and low surface tension represented the main features of self-cleaning coatings, and
e. sustainability and long-term stability of engineering graphene-based self-cleaning nanostructures.

7.2. Synthesis methods of Superhydrophobic biomimetic surfaces

Improving the hydrophobic properties of nanostructured biomimetic surfaces by using controlled nanofiller-matrix composite provides low-cost, functionality, self-cleaning and robustness. In turn, agglomeration and low distribution of nanofillers reduce the design features and self-cleaning characteristics. Enhancement of nanofiller distribution in the matrix by using polymers is based on selection of suitable synthesis method. Deposition of polymeric compounds on graphene-hybrid metal oxide may resist the graphene aggregation and afford a superhydrophobic nanocomposite layer with micro-/nano-roughness. Recently, many elegant routes have been applied to prepare superhydrophobic biomimetic surfaces, as mentioned in **Table 3**.[232-238] Table 3 represents different techniques for fabrication of ultrahydrophobic nano-surfaces and illustration of their merits and defects.

Table 3

Controlling and exploiting surface roughness are important to engineer superhydrophobicity. Although, studies elucidated the micro-scale roughness features and the nanoscale structures, there is lack a full understanding of the non-wettability on hybrid inorganic nanocomposites. These hybrid nanofillers are efficient to cause surface roughness of the nanocomposites, improving the surface hydrophobicity and self-cleaning features. Silicone-containing block copolymer structures can provide high mechanical durability and obviate the poor mechanical properties that are reported with PDMS homopolymers. A well-dispersion of nanofillers in the copolymer leads to increased matrix-nanofiller's interfacial bodings and the surface area to yield extra-ordinary and durable self-cleaning feature. Thus, surface micro-/nano-roughness generated by graphene/metal oxide hybrid nanocomposite can improve the nanocomposite.

Together, the increase in the solid–liquid interface of biomimetic surfaces will improve both the surface roughness and its hydrophobicity through entrapping air in the surface microgrooves. The design of densely-packed biomimetic nanocomposite layers enhances the surface micro-/nano-roughness. The designed biomimetic products may have better global acceptance with a physical fouling-prevention mechanism, which can prevent surface micro-fouling bonding without toxicity.

8. Conclusions and final remarks

The continuous increase in the maritime navigation activities suggests a force-driven progress of effective and eco-friendly fouling-resistance surfaces. This review highlights on the progress of new fouling-prevention nanosurfaces for self-cleaing applications and engineered FR nano-surfaces. Various nanostructured hybrid composites/nanocomposite materials with unique physical, chemical and surface features have been developed through mimicking the natural self-cleaning surfaces for marine antifouling. The improved surface area, biocompatibility, and high distribution level of nanofillers in the polymeric matrix are key clues for engineering FR coatings. Suitably dispersed nanofillers in composite building blocks at different loading concentrations can modify the physico-mechanical and wetting behavior. Silicon-based superhydrophobic nanocomposites have been widely used to design self-cleaning nano-surfaces as an ecological fouling-prevention coating in the shipping industry. Silicone-containing block copolymer enriched with

graphene-metal oxide nanocomposites is the modern research gateway The subtle structural changes in the designed micro-/nano-binary composites provided outstanding self-cleaning and FR surfaces. These surfaces enabled air trapping within their grooves and between the water drops and coating layers. Optimized micro-textures on the nanocomposite building blocks retain the surface transformation from Cassie-Baxter to Wenzel model with improved ultrahydrophobicity. Thus, future directions for marine environmental security has motivated FR self-cleaning research toward new innovations:

(i) GO hybrid-1D nanomaterials (such as γ-Al_2O_3 and SiC nanowires) are promising to develop ternary nanocomposites of PDMS/GO-γ-Al_2O_3 nanorod (NR) surfaces with superhydrophobic self-cleaning and FR characteristics (Figure 17). Single crystal SiC NWs with a preferential (111) growth direction and γ-Al_2O_3 nanorods with (101) orientation can be employed as ceramic nanofillers. A simple one-phase method can be used to prepare these hybrid nanocomposites. These ternary building blocks can also improve the FR features and achieve high distribution of nanofillers in the polymeric matrix through their high surface area and physico-mechanical features. Simplicity, cost-savings, environmental impacts, robustness, and self-cleaning FR coating features are attractive merits of this nanocomposite.

Figure 17

(ii) Controlled-synthesis of nanofillers with special morphologies, tectonic building blocks, hierarchal architectures, and surface interfaces will provide significant antifouling surfaces.
(iii) The nanofiller surface heterogeneity, anisotropy and complexity will function the coating's hydrophobicity and lead to develop a smart surface with reversible tuneable features.
(iv) Silicone-containing block copolymers as FR coatings may exhibit non-leachant property and stability in water.
(v) Various modified PDMS-polyurethane, PDMS-epoxy, and PDMS-fluorinated copolymers should be developed with surface functionality.
(vi) Anchoring rGO surface with metal oxide photocatalysts will offer a green environment to provide coatings with self-cleaning and fouling resistance features.
(vii) Advanced biomimetic superhydrophobic nanocomposite surfaces may provide multifunctional surfaces for FR, self-cleaning, and anticorrosion features.

Overall, fouling-resistant coatings based on ternary and quaternary nanostructured composites are promising fields for further study because of their high diversity. The nanoscale function models in terms of small-size nano-fabrication, low energy consumption, smart dynamic movements, chemical/electrical diffusions, transports, conductivity, electronics and optics may open a modern research gateway for development of cutting-edge environmental clean-up systems, which are the core of building super-smart society.

Notes and references

[1] M. S. Selim, M. A. Shenashen, S. A. El-Safty, M. Sakai, S. A. Higazy, M. M. Selim, H. Isago, A. Elmarakbi, *Prog. Mater. Sci.,* 2017, **87**, 1-32.
[2] W. J. Yang, K-G. Neoh, E-T. Kang, SL-M. Teo, D. Rittschof, *Prog. Polym. Sci.*, 2014, **39**, 1017-1042.
[3] S. Krishnan, C. J. Weinman, C. K. Ober, *J. Mater. Chem.*, 2008, **18**, 3405-3413.
[4] (a) M. S. Selim, S. A. El-Safty, M. A. El-Sockary, A. I. Hashem, O. M. Abo Elenien, A. M. EL-Saeed, N. A. Fatthallah, *Mater. Des.*, 2016, **101**, 218-225; (b) C. Howell, T. L. Vu, J. J. Lin, S. Kolle, N. Juthani, E. Watson, J. C. Weaver, J. Alvarenga, J. Aizenberg, *ACS Appl. Mater. Interfaces*, 2014, **6 (15)**, 13299–13307; (c) B. K. Nayak, P. O. Caffrey, C. R. Speck, M. C. Gupta, *Appl. Surf. Sci.*, 2013, **266**, 27-32.
[5] J. Wang, X. Jin, C. Li, W. Wang, H. Wu, S. Guo, *Chem. Engin. J.,* 2019, **370**, 831-854.
[6] 1)H. Khalifa, S. A. El-Safty, A. Reda, M. A. Shenashen, M. M. Selim, A. Elmarakbi H. A. Metawa, *Nano-Micro Letters* 2019, **11**, 84; (b) H. Khalifa, S. A. El-Safty, A. Reda, M. A. Shenashen, M. M. Selim, O. Y. Alothman, N. Ohashi, *Sci. Rep*., 2019, **9**, 14701; (c) H. Gomaa, M. A. Shenashen, H. Yamaguchi, A. S. Alamoudi, S. A. El-Safty, *Green Chem*., 2018, **20**, 1841-1857
[7] (a)A.M. Azzam, M. A. Shenashen, M. M. Selim, H. Yamaguchi, I.M. ElSewify, S. Kawada, A. A. Alhamid, S.A. El-Safty, *J. Phys. Chem. Solids*, 2017, **109**, 78-88; (b)A.M. Azzam, M. A. Shenashen, M.M. Selim, A.S. Alamoudi, S.A. El-Safty, *ChemistrySelect*, 2017, **2(35)**, 11431-11437
[8] S-H. Kim, S. Lee, D. Ahn, J. Y. Park, *Sens. Actuators* B-*Chem.*, 2019, **293**, 115-121.
[9] (a) M. S. Selim, H. Yang, F. Q. Wang, N. A. Fatthallah, X. Li, Y. Li, Y. Huang, *J. Coat. Technol. Res.*, 2019, 1-16; (b) M. S. Selim, S. A. El-Safty, M. A. El-Sockary, A. I. Hashem, O. M. Abo Elenien, A. M. EL-Saeed, N. A. Fatthallah, *Data in Brief,* 2016, **8**, 1357-1364.
[10] A. Elbourne, R. J. Crawford, E. P. Ivanova, *J. Colloid. Interface Sci.*, 2017, **508**, 603-616.
[11] H. K. Webb, R. J. Crawford, E. P. Ivanova, *Adv. Colloid. Interface Sci.*, 2014, **210**, 58-64.
[12] (a) L. Zhai, F. C. Cebeci, R. E. Cohen, M. F. Rubner, *Nano Letters* 2004, ***4, 7,*** 1349-1353; (b) Y. Liu, S. Li, J. Zhang, J. Liu, Z. Han, L. Ren, *Corrosion Sci*. 2015, **94**, 190-196
[13] M. Ma, R.M. Hill, *Curr. Opin. Colloid Interface Sci.*, 2006, **11**, 193–202.
[14] E. Martines, K. Seunarine, H. Morgan, N. Gadegaard, C. D. W. Wilkinson, M. O. Riehle, *Nano Lett.*, 2005, **Bd. 5**, 2097–2103.
[15] (a) T. Onda, S. Shibuichi, N. Satoh, K. Tsujii, *Langmuir*, 1996, **12**, 2125–2127. (b) H. Gomaa, M.A. Shenashen, H. Yamaguchi, A.S. Alamoudi, M. Abdelmottaleb, M.F. Cheira, T.A. Seaf El-Naser, S.A. El-Safty, *J. Clean. Prod.*, 2018, **182**, 910–925; (c) A. Derbalah, S.A. El-Safty, M.A. Shenashen, M. Khairy, *ChemPlusChem*., 2015, **80 (12)**, 1769–1778; (d) N. Akhtar, M.Y. Emran, M.A. Shenashen, H. Khalifa, T. Osaka, A. Faheem, T. Homma, H. Kawarada, S.A. El-Safty, *J. Mater. Chem. B*., 2017, **5 (39)**, 7985–7996.
[16] (a) D. Hassen, M. A. Shenashen, S. A. El-Safty, M. M. Selim, H. Isago, A Elmarakbi, A El-Safty, H Yamaguchi, *J. Power Sources,* 2016, **330**, 292-303; (b) S.A. El-Safty, M Sakai, M. M. Selim, A. A. Alhamide, *RSC Adv.,* 2015, **5 (74),** 60307-60321.
[17] (a) M. Y. Emran, M. A. Shenashen, H. Morita, S. A. El-Safty, *Adv. Healthcare Mater.* 2018, **7 (16),** 1701459; (b) T. Balaji, S. A. El-Safty, T. Hanaoka, H. Matsunaga, F. Mizukami, *Angew. Chem. Int. Ed.* 2006, **45**, 7202-7208.
[18] (a) S. A. El-Safty, M. A. Shenashen , M. Ismael , and M. Khairy, *Adv. Funct. Mater.* 2012, **22**, 3013–3021; (b) M.S. Selim, P.J. Mo, Y.P. Zhang, Z. Hao, H. Wen, *Ceramic Inter.* 2020, (In press, https://doi.org/10.1016/j.ceramint.2019.12.183).
[19] D. Hassen, M. A. Shenashen, A. R. El-Safty, A. Elmarakbi, S. A. El-Safty, *Sci. Rep.* 2018, **8**, 3740.
[20] (a) X. Gao, Z. Guo, *J. Bionic Engineering*, 2017, **14**, 401–439; (b) J. W. Woodward, H. Gwin, D. K. Schwartz, *Langmuir*, 2000, **16 (6)**, 2957–2961.
[21] M. Ma, Y. Mao, M. Gupta, K. K. Gleason, G. C. Rutledge, *Macromolecules*, 2005, **38 (23)**, 9742–9748.
[22] M. S. Selim, S. A. El-Safty, A. M. Azzam, M. A. Shenashen, M. A. El-Sockary, O. M. Abo Elenien, *ChemistrySelect*, 2019, **4**, 3395–3407.
[23] A. Nakajima, K. Hashimoto, T. Watanabe, *Monatsh. Chem.*, 2001, **132**, 31–41
[24] C. Dong, Y. Gu, M. Zhong, L. Li, K. Sezer, M. Ma, W. Liu, *J. Mater. Process. Technol.*, 2011, **211 (7)**, 1234–1240.
[25] A. G. Nurioglu, A. C.C. Esteves, G. de With, *J. Mater. Chem. B.,* 2015, **3**, 6547-6570.
[26] (a) M. S. Selim, S. A. El-Safty, M. A. Shenashen, Chapter 8 - Superhydrophobic foul resistant and self-cleaning polymer coating, In: Superhydrophobic Polymer Coatings, (Eds. S. K. Samal, S. Mohanty, S. K. Nayak,) (Elsevier Scientific Publisher Company, New York, 2019, 181-203); (b) A. M. Elseman, M. S. Selim, L. Luo, C. Y. Xu, G. Wang, Y. Jiang, D. B. Liu, L.P. Liao, Z. Hao, Q. Song, *ChemSusChem*, 2019, **12**, 1 – 10.
[27] X. Li, M.A. Shenashen, X. Wang, A. Ito, A. Taniguchi, S. A. El-Safty, *Sci. Rep.* 2017, **7,** 16749.
[28] Y. B. Zhang, Y. W. Tan, H. L. Stormer, P. Kim, *Nature*, 2005, **438**, 201-204.
[29] (a) S. Berber, Y. Kwon, D. Tománek, *Phys. Rev. Lett.*, 2000, **84**, 4613-4616; (b) E. Brown, L. Hao, J. C. *Appl. Phys. Lett.* 2005, **87**, 023107, (c) M. Freitag, M. Steiner, Y. Martin, V. Perebeinos, Z. Chen, J. C. Tsang, P. Avouris, *Nano Lett*. 2009, **9(5)**, 1883-1888

[30] (a) S. Pattnaik, K. Swain, Z. Lin, *J. Mater. Chem. B.,* 2016, **4**, 7813-7831; (b) M. Deng, Y. Huang, *Ceramics Int.,* 2020, **46(2)**, 2565-2570; (c) J. Hu, J. Zhu, S. Ge, C. Jiang, T. Guo, T. Peng, T. Huang, L. Xie, *Surface Coat. Tech.* 2020, 12536 (https://doi.org/10.1016/j.surfcoat.2020.12536.
[31] S. Banerjee, J. Shim, J. Rivera, X. Jin, D. Estrada, V. Solovyeva, X. You, J. Pak, E. Pop, N. Aluru, R. Bashir, *Acs Nano*, 2013, **7(1)**, 834-843.
[32] E. Singh, Z. Chen, F. Houshmand, W. Ren, Y. Peles, H.M. Cheng, N. Koratkar, *Small*, 2013, **9**, 75–80.
[33] D. A. Zha, S. Mei, Z. Wang, H. Li, Z. Shi, Z. Jin, *Carbon,* 2011, **49(15)**, 5166–5172.
[34] L. Zhang, N. Hu, C. Yang, H. Wei, Z. Yang, Y. Wang, L. Wei, Y. Zhang, *Compos. Part A: Appl. Sci. Manuf.*, 2015, **74**, 96–106.
[35] S. P. Cooper, J. A. Finlay, G. Cone, M. E. Callow, J. A. Callow, A. B. Brennan, *Biofouling*, 2011, **27**, 881–91.
[36] E. K. Sam, D. K. Sam, X. Lv, B. Liu, X. Xiao, S. Gong, W. Yu, J. Chen, J. Liu, *Chem. Eng. J.,* 2019, **373**, 531-546.
[37] M. P. Schultz, J. A. Bendick, E. R. Holm, W. M. Hertel, *Biofouling*, 2010, **27(1)**, 87–98.
[38] D. Carteaua, K. Vallèe-Rèhela, I. Linossier, F. Quiniou, R. Davy, C. Compère, M. Delbury and F. Faÿ, *Prog. Org. Coat.,*2014, **77(2)**, 485–493.
[39] H.G. Silverman, F.F. Roberto, Mar. *Biotechnol.* 2007, **9**, 661–81.
[40] J-P. Maréchal, C. Hellio, *Int. J. Mol. Sci.*, 2009, **10(11)**, 4623–4637.
[41] E. D. Van Hullebusch, M. H. Zandvoort, P. N. L. Lens, *Rev. Environ. Sci. Biotechnol.*, 2003, **2(1)**, 9-33.
[42] M. Aslam, R. Ahmad, J. Kim, *Sep. Purif. Technol.,* 2018, **206**, 297-315.
[43] M. R. Detty, R. Ciriminna, F.V. Bright, M. Pagliaro, *Acc. Chem. Res.*, 2014, **47 (2)**, 678–687.
[44] C. Compere, M. N. Bellon-Fontaine, P. Bertrand, D. Costa, P. Marcus, C. Poleunis, *Biofouling*, 2001, **17**, 129–145.
[45] S. Soroldoni, Í. B. Castro, F. Abreu, F. A. Duarte, R. B. Choueri, O. O. Möller, G. Fillmann, G. L. L. Pinho, *Water Res.,* 2018, **137**, 47-56.
[46] N. D. Hoa, S. A. El-Safty, *Chem–Eur J.*, 2011, **17(46)**, 12896–12901.
[47] L. Xue, X. Lu, H. Wei, P. Long, J. Xu, Y. Zheng, *J. Colloid Interface Sci.,* 2014, **421**, 178–183.
[48] M. P. Schultz, *Biofouling,* 2007, **23**, 331–341.
[49] I. Cheyne, Regulation of marine antifouling in international and EC law. In: S. Dürr and J. C. Thomason (eds) Biofouling. Wiley-Blackwell, Chichester. 2010, 306–318.
[50] P. M. Imbesi, N. V. Gohad, M. J. Eller, B. Orihuela, D. Rittschof, E. A. Schweikert, A. S. Mount, K. L. Wooley *ACS Nano,* 2012, **6(2)**, 1503–1512.
[51] U. Eduok, O. Faye, J. Szpunar, *Prog. Org. Coat.,* 2017, **111**, 124-163.
[52] L. Tamayo, M. Azócar, M. Kogan, A. Riveros, M. Páez, *Mater. Sci. Engin. C,* 2016, **69**, 1391-1409.
[53] A. Elbourne, R. J. Crawford, E. P. Ivanova, *J. Colloid Interface Sci.*, 2017, **508**, 603-616.
[54] M. Legg, M.K. Yücel, I. Garcia de Carellan, V. Kappatos, C. Selcuk, T.H. Gan, *Ocean Engineering*, 2015, **103**, 237-247.
[55] C. Anderson, M. Atlar, M. Callow, M. Candries, A. Milne, R. L. Townsin, *J. Mar. Des. Oper.,* 2003, **B4**, 11–23.
[56] M. Awais, A. A. Bhuiyan, *Int. J. Heat Mass Transfer,* 2019, **41**, 580-603,
[57] T. Akinfiev, A. Janushevskis, E. Lavendelis, *Trans. & Engin. Mechan.*, 2007, **6(24)**, 133 -145.
[58] S. A. Umoren, M. M. Solomon, *Prog. Mater. Sci.,* 2019, **104**, 380-450.
[59] Q. Xie, J. Pan, C. Ma, G. Zhang, *Soft Mater,* 2019, **15**, 1087—1107.
[60] E. Almeida, T. C. Diamantino, O. de Sousa, *Prog. Org. Coat.*, 2007, **59**, 2–20.
[61] M. E. Callow, J. A. Callow, *Biologist*, 2002, **49 (1)**, 10.
[62] Marmur A. *Langmuir,* 2004, **20**, 3517–3519.
[63] M.L. Carman, T.G. Estes, A.W. Feinberg, J.F. Schumacher, W. Wilkerson, L.H. Wilson, M.E. Callow, J.A. Callow, A.B. Brenan, *Biofouling,* 2006, **22 (1)**, 11.
[64] P. Peng, N.H. Voelcker, S. Kumar, H.J. Griesser, *Biointerphases*, 2007, **2 (2)**, 95-104.
[65] C. M. Magin, S. P. Cooper, A. B. Brennan, *Mater. Tod.*, 2010, **13 (4)**; 36-44.
[66] M. Ferrari, A. Benedetti, *Adv. Coll. Interf. Sci.* 2015, **222**, 291–304.
[67] S. Tian, D. Jiang, J. Pu, X. Sun, Z. Li, B. Wu, W. Zheng, W. Liu, Z. Liu, *Chem. Engin. J.*, 2019, **370**, 1-9.
[68] (a) K. A. Dafforn, J. A. Lewis, E. L. Johnston, *Mar. Pollut. Bull.*, 2011, **62**, 453–465; (b) S. Kiil, C. E. Weinell, M. S. Pedersen, K. Dam-Johansen, *Indust. Eng. Chem. Res.* 2001, **40(18)**, 3906–3920.
[69] S. Nir, M. Reches, *Curr. Opin. Biotechnol.,* 2016, **39**, 48-55.
[70] L. D. Chambers, K. R. Stokes, F. C. Walsh, R. J. K. Wood, *Surf. Coat. Technol.*, 2006, **201**, 3642-3652.
[71] Y. Sapozhnikova, E. Wirth, K. Schiff, M. Fulton, *Mar. Pollut. Bull.* 2013, **69(1– 2)**, 189–194.
[72] Y. Li, C. Ning, *Bioact. Mater.,* 2019, **4**, 189-195.
[73] D. M. Yebra, S. Kiil, K. Dam-Johansen, *Prog. Org. Coat.,* 2004, **50**, 75–104;
[74] M. S. Acevedo, C. Puentes, K. Carreño, J. G. León; M. Stupak, M. García, M. Pérez, G. Blustein, *Inter. Biodeter. Biodegrad.,* 2013, **83**, 97-104.
[75]M. Salta, J. A. Wharton, P. Stoodley, S. P. Dennington, L.R. Goodes, S. Werwinski, U. Mart, R.J.K. Wood, K.R. Stokes, *Philos. Trans. R Soc. A*. 2010, **368**, 4729–4754.
[76]B. Sharma, P. Malik, P. Jain, *Mater. Tod. Commun.,* 2018, **16**, 353-363.
[77]M-L. Kung, P-Y. Lin, S-W. Peng, D-C. Wu, W-J. Wu, B-W. Yeh, M-H. Tai, H-S. Hung, S. Hsieh, *Appl. Mater. Tod.,* 2016, **4**, 31-39.
[78] X. Han, D.Y. Zhang, X. Li, et al., *Chin. Sci. Bull.* 2008, **53**, 1587–1592
[79] X.Q. Bai, G.T. Xie, H. Fan, Z.X. Peng, C.Q. Yuan, X.P. Yan ,*Wear*, 2013, **306 (1–2)**, 285-295.
[80] T. Zeng, P. Zhang, X. Li, Y. Yin, K. Chen, C. Wang, *Appl. Surf. Sci.,* 2019, **493**, 1004-1012.
[81] J. Chenw, C. L. Brooks, *Phys. Chem. Chem. Phys.*, 2008, **10**, 471–481.
[82] B. Mockenhaupt, H-J. Ensikat, M. Spaeth, W. Barthlott, *Langmuir*, 2008, **24 (23)**, 13591–13597.
[83] G. Wang, Z. Guo, W. Liu, *J. Bionic Engin.* 2014, **11**, 325–345.
[84] T. Sun, L. Feng, X. Gao, L. Jiang, *Acc. Chem. Res.*, 2005, **38 (8)**, 644–652.
[85] X. Zheng, S. Fu, *Colloid. Surf. A Physicochem. Eng. Asp.,* 2019, **560,** 171-179.
[86] B. Bhushan, Y. C. Jung, *Prog. Mater. Sci.*, 2011, **56 (1)**, 1-108.
[87] H. Gundersen, H. P. Leinaas, C. Thaulow, *Beilstein. J. Nanotechnol.* 2017, **8**, 1714–1722.
[88] Y. Zheng, X. Gao, L. Jiang, *Soft Matter*, 2007, **3**, 178–182.
[89] (a) G. D. Bixler, B. Bhushan, *Soft Matter*., 2012, **8**, 11271–11284; (b) M. A. Shenashen, D. Hassen, S. A. El-Safty, H. Isago, A. Elmarakbi, H. Yamaguchi, *Chem. Eng. J.*, 2017, **313**, 83–98.
[90] (a) E. Celia, T. Darmanin, D. T. de Givenchy, S. Amigoni, F. Guittard, *J. Colloid Interface Sci.* 2013, **402**, 1-18; (b) H. Cao, Q. Yu, R. Colby, D. Pandey, C. S. Park, J. Lian, D. Zemlyanov, I. Childres, V. Drachev, E.A. Stach, M. Hussain, H. Li, S. S. Pei, Y. P. Chen, *J. Appl. Phys.* 2010, **107**, 044310–044317.
[91] X. F. Gao, L. Jiang, *Nature*, 2004, **432**, 36.
[92] L. Feng, Y. Zhang, J. Xi, J. Xi, Y. Zhu, N. Wang, F. Xia, L. Jiang, *Langmuir*, 2008, **24**, 4114–4119.
[93] H. Zhang, X. Lu, Z. Xin, W. Zhang, C. Zhou, *Prog Org. Coat*., 2018; **123**: 254-260.
[94] G. D. Bixler, A. Theiss, B. Bhushan, S. C. Lee, *J. Colloid Interface Sci.*, 2014, **419**, 114–133.
[95] D. Bechert, M. Bruse, W. Hage, *Exp. Fluids,* 2000, **28 (5)**, 403–412.
[96] M. Wouters, C. Rentrop, P. Willemsen, *Prog. Org. Coat.*, 2010, **68**, 4-11.
[97] Y. Luan, S. Liu, M. Pihl, H. C. van der Mei, J. Liu, F. Hizal, C-H. Choi, H. Chen, Y. Ren, H. J. Busscher, *Curr. Opinion Colloid. Interface Sci.,* 2018, **38**, 170-189.
[98] F. Wan, X. Pei, B. Yu, Q. Ye, F. Zhou, Q. Xue, *ACS Appl. Mater. Interfaces* 2012, **4(9)**, 4557–4565.
[99] G. G. Sankar, S. Sathya, P. S. Murthy, A. Das, R. Pandiyan, V. B. Venugopalan, M. Doble, *Inter Biodetor. Biodegrad.*, 2015, **104**, 307-314.
[100] K. J. Wynne, G. W. Swain, R. B. Fox, S. Bullock, J. Uilk. *Biofouling*, 2000, **16**, 277–288.
[101] R. P. S. Chakradhar, V. D. Kumara, J. L. Raob, B. Bharathibai, *J. Appl. Surf. Sci.*, 2011, **257**, 8569-8575.
[102] J. Chapman, F. Regan, *Adv. Eng. Mater.*, 2012, **14 (4)**, B175–B184.
[103] (a) M. S. Selim, A. Elmarakbi, A. M. Azzam, M. A. Shenashen, A. M. EL-Saeed, S. A. El-Safty, *Prog. Org. Coat.*, 2018, **116**, 21-34; (b) M. A. Shenashen, N. Akhtar, M. M. Selim, W. M. Morsy, H. Yamaguchi, S. Kawada, A. A. Alhamid, N. Ohashi, I. Ichinose, A. S. Alamoudi, S. A. El-Safty, *Chem. Asian J.*, 2017, **12 (15)**, 1952–1964; (c) S. A. El-Safty, M. Sakai, M. Selim, A. A. Hendi, *ACS Appl. Mater. Interfaces*, 2015, **7 (24)**, 13217–13231.
[104] (a) M. A. Shenashen, D. Hassen, S. A. El-Safty, N. Akhtar, A. Chatterjee, A. Elmarakbi, *Adv. Mater. Interfaces*, 2016, **3(24)**, 1600743; (b) M. Y Emran, S. A. El-Safty, M. A. Shenashen, T Minowa, *Sens. Actuat. B-Chem.*, 2019, **284**, 456-467.

[105] C-H. Xue, S-T. Jia, J. Zhang, L. Q. 2019, H. Z. Chen, M. Wang, *Sci. Technol. Adv. Mater.*, 2008, **9 (3)**, 035008.
[106] M. S. Selim, S. A. El-Safty, M. A. El-Sockary, A. I. Hashem, O. M. Abo Elenien, A. M. EL-Saeed, N. A, Fatthallah, *RSC Adv.*, 2015, **5(78)**, 63175-63185.
[107] M. S. Selim, S. A. El-Safty, M. A. El-Sockary, A. I. Hashem, O. M. Abo Elenien, A. M. EL-Saeed, N. F. Fatthallah, *Mater. Des.*, 2016, **101**, 218-225.
[108] M. S. Selim, M. A. Shenashen, S. Hasegawa, N. A. Fatthallah, A. Elmarakbi, S. A. El-Safty, *Chem. Eng. J.*, 2017, **320**, 653-666.
[109] M. S. Selim, S. A. El-Safty, M. A. El-Sockary, A. I. Hashem, O. M. Abo Elenien, A. M. EL-Saeed, N. A. Fatthallah, *RSC Adv.*, 2015, **5 (26)**, 19933–19943.
[110] N. Durand, D. Mariot, B. Ame´duri, B. Boutevin, F. Ganachaud, *Langmuir*, 2011, **27 (7)**, 4057–4067.
[111] P. Buskens, M. Wouters, C. Rentrop, Z. Vroon, *J. Coat. Technol. Res.*, 2013, **10(1)**, 29–36.
[112] J. A. Callow, M. E. Callow, *Nat. Commun.*, 2011, **2**, 244-254.
[113] (a) A. di Biase, M. S. Kowalski, T. R. Devlin, J. A. Oleszkiewicz, *J. Environ. Manag.,* 2019, **247**, 849-866; (b) J. Millett, C. D. Anderson, Fighting fast ferry fouling, Fast '97, Conference papers, Vol. 1. Australia: Baird Publications; 1997.
[114] J. Stein, K. Truby , C. D. Wood , J. Stein, M. Gardner , G. Swain, C. Kavanagh, B. Kovach, M. Schultz , D. Wiebe, E. Holm, J. Montemarano, D. Wendt, C. Smith, A. Meyer, *Biofouling,* 2003; **19**, 71–82.
[115] T. Hanemann T, D. V. Szabo, *Materials,* 2010, **3(6)**, 3468–517.
[116] M. S. Selim, M. A. Shenashen, A. I. Hashem, S. A. El-Safty, *New J. Chem.*, 2018, **42**, 10048-10058.
[117] (a) A. Beigbeder, P. Degee, S. L. Conlan, R. Mutton, A. S. Clare, M. E. Pettitt, M. E. Callow, J. A. Callow, P. Dubois, *Biofuels* 2008, **24(4)**, 291–302; (b) M. A. Shenashen, A. Derbalah, A. Hamza, A. Mohamed, S.A. El Safty, *Pest Manag. Sci.*, 2017, **73 (6)**, 1121–1126; (c) A. Derbalah, S. A. El-Safty, M. A. Shenashen, N. Abdel Ghany, *ChemPlusChem,* 2015, **80 (7)**, 1119–1126; (d) S. A. El-Safty, M. A. Shenashen, M. Khairy, *Colloids Surf. B- Biointerfaces*, 2013, **103**, 288–297; (e) S. A. El-Safty, M. A. Shenashen, M. Ismael, M. Khairy, *Chem. Commun.*, 2012, **48**, 6708–6710.
[118] (a) M. Khairy, S. A. El-Safty, *Sens. Actuators* B, 2014, **193**, 644–52; (b) D Hassen, S. A. El-Safty, K Tsuchiya, A Chatterjee, A Elmarakbi, M A Shenashen, M Sakai, Sci. Rep., 2016, **6,** 24330; (c) X. Lia, M. A. Shenashen, X. Wang, A. Ito, A. Taniguchi, S.A. El-Safty, *Adv. Biosys.*, 2018, **2**, 1700114.
[119] (a) M.S. Selim, M.A. Shenashen, N.A. Fatthallah, A. Elmarakbi, S.A. El-Safty, *ChemistrySelect*, 2017, **30**, 9691–9700; (b) M. A. Shenashen, S. Kawada, M. M. Selim, W. M. Morsy, H. Yamaguchi, A. A. Alhamid, N. Ohashi, I. Ichinose, S. A. El-Safty, *Nanoscale*, 2017, **9**, 7947–7959; (c) A.-A. E. Soliman, M. A. Shenashen, I. M. El-Sewify, G. M. Taha, M. A. El-Taher, H. Yamaguchi, A. S. Alamoudi, M. M. Selim, S. A. El-Safty, *ChemistrySelect*, 2017, **2 (21)**, 6135–6142.
[120] (a) J. Stein, K. Truby, C. D. Wood, M. Takemori, M. Vallance, G. Swain, C. Kavanagh, B. Kovach, M. Schultz, D. Wiebe, D. Wendt, C. Smith, A. Meyer, *Biofouling*, 2003, **19(2)**, 87–94; (b) M. Y. Emran, H. Khalifa, H. Gomaa, M. A. Shenashen, N. Akhtar, M. Mekawy, A. Faheem, S.A. El-Safty, *Microchim. Acta*, 2017, **184 (11)**, 4553–4562.
[121] M. P. Wolf, G. B. Salieb-Beugelaar, P. Hunziker, *Prog. Polym. Sci.,* 2018, **83**, 97-134.
[122] (a) N. Roy, A. K. Bhowmick, *Polymer*, 2010, **51(22)**, 5172–85; (b) H. Murase, T. Fujibayashi, *Prog. Org. Coat*., 1997, **31**, 97–104.
[123] (a) J. Santaren, E. Ruiz-Hitzky, *Clays Clay Miner*, 1990, 38(1), 63–68; (b) M. Kotal, A. K. Bhowmick. *Prog Polym. Sci.* 2015, **51**, 127–87.
[124] E. Martinelli, M. Suffredini, G. Galli, A. Glisenti, M. E. Pettitt, M. E. Callow, D. Williams, G. Lyall, *Biofouling* 2011, **27(5)**, 529–41.
[125] M. Atlar, B. Ünal, U. O. Ünal, G. Politis, E. Martinelli, G. Galli, C. Davies, D. Williams, *Biofouling,* 2013, **29(1)**, 39–52.
[126] W. Zhang, Y. Zheng, L. Orsini, A. Morelli, G. Galli, E. Chiellini, E. E. Carpenter, K. J. Wynne, *Langmuir,* 2010, **26(8)**, 5848–55.
[127] C. M. Friesen, B. Améduri, *Prog. Poly. Sci.,* 2018, **81**, 238-280.
[128] X. Gou, Z. Guo, *Adv Colloid Interface Sci.,* 2019, **269**, 87-121.
[129] A. Giwa, S.W. Hasan, A. Yousuf, S. Chakraborty, D.J. Johnson, N. Hilal, *Desalination*, 2017, **420**, 403-424.
[130] Z. Han, Z. Mu, W. Yin, W. Li, S. Niu, J. Zhang, L. Ren, *Adv. Colloid. Interface Sci.,* 2016, **234**, 27-50.
[131] B. Y. Kim, L. Y. Hong, Y. M. Chung, D. P. Kim, *Adv. Funct. Mater.*, 2009, **19**, 3796–803.
[132] J. Kozakiewicz, I. Ofat, J. Trzaskowska, *Adv. Colloid. Interface Sci.,* 2015, **223**, 1-39.
[133] S. B. Ulaeto, R. Rajan, J. K. Pancrecious, T. P. D. Rajan, B. C. Pai, *Prog. Org. Coat.,* 2017, **111**, 294-314,
[134] J. S. Mohammed, *Prog. Oceanogr.,* 2015, **134**, 451-473.
[135] S. Ghaffari, M. Aliofkhazraei, Gh. Barati Darband, A. Zakeri, E. Ahmadi, *Surf. Interfaces,* 2019, **17**, 100340.
[136] E. Yilgor, I. Yilgor, *Prog. Polym. Sci.*, 2014, **39**, 1165–1195.
[137] R. Zhang, Y. Liu, M. He, Y. Su, X. Zhao, *Chem. Soc. Rev.*, 2016, **45**, 5888-5924.
[138] (a) M. S. Selim, A. Elmarakbi, A. M. Azzam, M. A. Shenashen, A. M. EL-Saeed, S.A. El-Safty, *Prog. Org. Coat*., 2018, **116**, 21–34; (b) N.A. Samak, M.S. Selim, Z. Hao, J. Xing, *Talanta*, 2020, **211**, 120655.
[139] S-J. Yang, X. Chen, B. Yu, H-L. Cong, Q-H. Peng, M.M. Jiao, *Integrated Ferroelectrics*, 2016, **169 (1)**, 29-34.
[140] X. H. Li, Z. Cao, Z. J. Zhang, H. X. Dang, *Appl. Surf. Sci.*, 2006, **252**, 7856-7861.
[141] M. S. Selim, M. A. Shenashen, A. Elmarakbi, A. M. ELSaeed, M. M. Selim and S. A. El-Safty, *RSC Adv.,* 2017, **7**, 21796–21808.
[142] (a) M.S. Selim, H. Yang, S.A. El-Safty, N.A. Fatthallah, M.A. Shenashen, F.Q. Wang, Y. Huang, Colloid. Surf. A Physicochem. Eng. Asp., 2019, **570**, 518–530; (b) M. S. Selim, Z. Hao, Y. Jiang, M. Yi, Y. Zhang, *Mater. Chem. Phys.,* 2019, **235**, 121733.
[143] (a) Y. Sun, Y. Ji, Y. Lang, L. Wang, B. Liu, Z. Zhang, *Inter. Biodeter. Biodegrad.*, 2018, **129**, 195-201; (b) S.K. Das, S. A. El-Safty, *ChemCatChem* 2013, **5**, 3050-3059; (c) S. A. El-Safty, A. Shahat, W.Warkocki, M. Ohnuma, *Small,* 2011, **7**, 62-65; (d) A. M. Azzam, M. A. Shenashen, B. B. Mostafa, W. A. Kandeel, S. A. El-Safty, *Environ. Prog. Sustain. Energy,* 2019, **38**, S260-S266.
[144] (a) H. Jin, T. Zhang, W. Bing, S. Dong, L. Tian, *J. Mater. Chem. B,* 2019, **7**, 488-497; (b) A. B. D. Cassie, S. Baxter, *Trans. Faraday Soc.*, 1944, **40**, 546–551.
[145] Z-H. Zhang, H-J. Wang, Y-H. Liang, X-J. Li, L-Q. Ren, Z-Q. Cui, C. Luo, *Sci Rep.*, 2018, **8**, 3869-3874.
[146] M. S. Selim, S. A. El-Safty, N. A. Fatthallah, M. A. Shenashen, *Prog. Org Coat.*, 2018, **121**, 160-172.
[147] P. Majumdar, E. Lee, N. Patel, S.J. Stafslien, J. Daniels, B.J. Chisholm, *J. Coat. Technol. Res.,* 2008, **5 (4)**, 405–417.
[148] S. S. Latthe, R. S. Sutar, V. S. Kodag, A. K. Bhosale, A. M. Kumar, K. K. Sadasivuni, R. Xing, S. Liu, *Prog. Org. Coat.,* 2019, **128**, 52-58.
[149] H. S. Abid, D. J. Johnson, R. Hashaikeh, N. Hilal, *Desalination,* 2017, **420**, 384-402,
[150] A. Terlizzi, M. Faimali,, Fouling on artificial substrata. In Dürr, S. and Thomason, J.C. (eds) Biofouling. Oxford: Wiley-Blackwell, 2010, 170–184.
[151] M-J. Na, H. Yang, H-J. Jung, S-D. Park, *Surf. Coat. Technol.*, 2019, **372**, 134-139.
[152] F. F. Estarlich, S. Lewey, T. Nevell, A. Thorpe, J. Tsibouklis, A. Upton, *Biofouling*, 2000, **16**, 263-275.
[153] J. E. Gittens, T. J. Smith, R. Suleiman, R. Akid, *Biotechnol. Adv.,* 2013, **31(8)**, 1738-1753.
[154] M. Zahid, G. Mazzon, A. Athanassiou, I. S. Bayer, *Adv. Colloid. Interface Sci.,* 2019, **270**, 216-250.
[155] S. A. Wilson, R. P.J. Jourdain, Q. Zhang, R. A. Dorey, C. R. Bowen, M. Willander, Q. U. Wahab, M. Willander, S. M. Al-hilli, O. Nur, E. Quandt, C. Johansson, E. Pagounis, M. Kohl, J. Matovic, B. Samel, W. van der Wijngaart, E. W. H. Jager, D. Carlsson, Z. Djinovic, M. Wegener, C. Moldovan, R. Iosub, E. Abad, M. Wendlandt, C. Rusu, K. Persson, *Mater. Sci. Engin. R Rep.,* 2007, **56 (1-6)**, 1-129.
[156] C. Stevens, D. E. Powell, P. Makela, C. Karman, *Mar. Pollut. Bull.*, 2001, **42**, 536-543.
[157] M. Nendza, *Mar. Pollut. Bull.*, 2007, **54**, 1190-1196.
[158] K. Truby, C. Wood, J. Stein, J. Cella, J. Carpenter, C. Kavanagh, G. Swain, D. Wiebe, D. Lapota, A. Meyer, E. Holm, D. Wendt, C. Smith, J. Montemarano, *Biofouling,* 2000, **15**, 141-150.
[159] A. Meyer, R. Baier, C. D. Wood, J. Stein, K. Truby, E. Holm, J. Montemarano, C. Kavanagh, B. Nedved, C. Smith, G. Swain, D. Wiebe, *Biofouling*, 2006, **22**, 411-423.
[160] B. T. Watermann, B. Daehne, S. Sievers, R. Dannenberg, J. C. Overbeke, J. W. Klijnstra, O. Heemken, *Chemosphere,* 2005, **60**, 1530-1541.
[161] F. Farjadian, M. Moghoofei, S. Mirkiani, A. Ghasemi, N. Rabiee, S. Hadifar, A. Beyzavi, M. Karimi, M. R. Hamblin, *Biotechnol. Adv.,* 2018, **36 (4)**, 968-985.

[162] M. Lejars, A. Margaillan, C. Bressy, *Chem. Rev.*, 2012, **112**, 4347–4390.
[163] C. Liu, Q. Xie, C. Ma, G. Zhang, *Ind. Eng. Chem. Res.*, 2016, **55**, 6671−6676.
[164] F. Irani, A. Jannesari, S. Bastani, *Prog. Org. Coat.*, 2013, **76**, 375–383.
[165] H. Y. Erbil, C. E. Cansoy, *Langmuir*, 2009, **25 (24)**, 14135–14145.
[166] Y-C. Pu, H-Y. Chou, W-S. Kuo, K-H. Wei, Y-J. Hsu, *Appl. Catal. B: Environ.*, 2016, **204**, 21-32.
[167] M.S. Selim, N.A. Samak, Z. Hao, J. Xing, *Mater. Chem. Phys.* 2020, **239**, 122300.
[168] I. R. Durán, G. Laroche, *Prog. Mater. Sci.,* 2019, **99**, 106–186; (b) A. Marmur, *Biofouling*, 2006, **22**, 107–115.
[169] C. J. Kavanagh, G. W. Swain, B. S, Kovach, J. Stein, C. Darkangelo-Wood, K. Truby, E. Holm, J. Montemarano, A. Meyer, D. Wiebe, *Biofouling*, 2003, **19(6)**, 381–390.
[170] M. S. Selim, H. Yang, Y. Li, F. Q. Wang, X. Li, Y. Huang, *Prog. Org. Coat.*, 2018, **120**, 217–227.
[171] R. Blossey, *Nature Mater.*, 2003, **2**, 301–306.
[172] M. S. Selim, F. Q. Wang, H. Yang, Y. Huang, S. Kuga, *Mater. Des.*, 2017, **135**, 173-183.
[173] F. Mumm, A. T. J. van Helvoort, P. Sikoski, *ACS Nano.*, 2009, **3(9)**, 2647-2652.
[174] J. L. Zhang, W. H. Huang, Y. C. Han, *Langmuir*, 2006, **22(7)**, 2946–2950.
[175] J-Y Shiu, C-W. Kuo, P. Chen, C-Y. Mou. *Chem Mater.,* 2004, **16 (4)**, 561–564.
[176] H. Yabu, M. Shimomura, *Chem. Mater.*, 2005, **17(21)**, 5231-5234.
[177] M. S. Selim, H. Yang, F. Q. Wang, X. Li, Y. Huang, N. A. Fatthallah, *RSC Adv.,* 2018, **8**, 9910–9921.
[178] S. K. Vashist, J. H. T. Luong, *Carbon*, 2015, **84**, 519–550.
[179] V. A. Ganesh, H. K. Raut, A. S. Nair, S. Ramakrishna, *J. Mater. Chem.*, 2011, **21**, 16304-16322.
[180] M. S. Selim, H. Yang, F. Q. Wang, N. A. Fatthallah, Y. Huang, S. Kuga, *Appl. Surf. Sci.,* 2019, **466**, 40–50.
[181] X. Zhao, Y. Li, B. Li, T. Hu, Y. Yang, L. Li, J. Zhang, *J. Colloid Interface Sci.,* 2019, **542**, 8-14.
[182] A. J. Scardino, H. Zhang, D. J. Cookson, R. N. Lamb, R. de Nys, *Biofouling*, 2009, **25(8)**, 757–767.
[183] D. G. Papageorgiou, I. A. Kinloch, R. J. Young, *Carbon*, 2015, **95**, 460-484.
[184] J. Liang, Y. Huang, L. Zhang, Y. Wang, Y. Ma, T. Guo and Y. Chen, *Adv. Funct. Mater.*, 2009, **19**, 2297–2302.
[185] N. D. Luong, U. Hippi, J. T. Korhonen, A. J. Soininen, J. Ruokolainen, L-S. Johansson, J-D. Nam, L. H. Sinh, J. Seppälä, *Polymer*, 2011, **52**, 5237–5242.
[186] S. Zinadini, A. A. Zinatizadeh, M. Rahimi, V. Vatanpour, H. Zangeneh, *J. Membrane Sci.*, 2014, **453**, 292–30.
[187] X. Wang, B. Ding, J. Yub, M. Wang, *Nano Tod.,* 2011, **6**, 510-530.
[188] A. Ambrosi, C. K. Chua, A. Bonanni, M. Pumera, *Chem. Rev.*, 2014, **114**, 7150–7188.
[189] **(a)** M. Y. Emran, M. Mekawy, N. Akhtar, M. A. Shenashen, I. M. EL-Sewify, A. Faheem, S. A. El-Safty, *Biosens. Bioelectron.,* 2018, **100**, 122–131; (b) M-F. Li, Y-G Liu, G-M. Zeng, N. Liu, S-B. Liu, *Chemosphere,* 2019, **226**, 360-380; (c) F. Duan, Y. Liao, Z. Zeng, H. Jin, L. Zhou, Z. Zhang, Z. Su, *Compos. Sci. Technol.,* 2019, **174**, 42-49.
[190] K. Krishnamoorthy, K. Jeyasubramanian, M. Premanathan, G. Subbiah, H. S. Shin, S. J. Kim, *Carbon*, 2014, **72**, 328 – 337.
[191] C. H. Chang, T. C. Huang, C. W. Peng, T. C. Yeh, H. I. Lu, W. I. Hung, J-M. Yeh, *Carbon*, 2012, **50**, 5044–5051.
[192] M. J. Nine, M. A. Cole, L. Johnson, D. N. H. Tran, D. Losic, *ACS Appl. Mater. Interfaces*, 2015, **7**, 28482−28493.
[193] H. Zhao, S. Chen, X. Quan, H. Yu, H. Zhao, *Appl. Catal. B.*, 2016, **194**, 134–140.
[194] M. Zhang, R. W. Field, K. Zhang, *J. Membr. Sci.*, 2014, **471**, 274–284.
[195] Y. Hong, Z. Wang, X. Jin, *Sci. Rep.*, 2013, **3**, 3439-3444.
[196] H-Y. He, *Mater. Sci. Semicon. Proc.,* 2015, **31**, 200–208.
[197] S. B. Rizvi, S.Y. Yang, M. Green, M. Keshtgar, A.M. Seifalian, *Bioconjug. Chem.,* 2015, **26 (12)**, 2384–2396.
[198] L-F. Ren, F. Xia, J. Shao, X. Zhang, J. Li, *Desalination*, 2017, **404**, 155–166.
[199] B. You, N. Wen, S. Zhou, L. Wu, D. Zhao, *J. Phys. Chem. B.*, 2008, **112 (26)**, 7706–7712.
[200] B. Das, K. E. Prasad, U. Ramamurty, C. N. R. Rao, *Nanotechnol.,* 2009, **20**, 125705.
[201] P. Song, Z. Cao, Y. Cai, L. Zhao, Z. Fang, S. Fu, *Polymer*, 2011, **52 (18)**, 4001-4010.
[202] M. F. Casula, A. Corrias, A. Falqui, V. Serin, D. Gatteschi, C. Sangregorio, C. de Julián Fernández, G. Battaglin, *Chem. Mater.*, 2003, **15 (11)**, 2201–2207.
[203] S. Nagarajan, M. Mohana, P. Sudhagar, V. Raman, T. Nishimura, S. Kim, Y. S. Kang, N. Rajendran, *ACS Appl. Mater. Interfaces*, 2012, **4 (10)**, 5134–5141
[204] M. Bassyouni, M. H. Abdel-Aziz, M. S. Zoromba, S. M. S. Abdel-Hamid, E. Drioli, *J. Indust. Eng. Chem.,* 2019, **73**, 19-46.
[205] P. Nguyen-Tri, H. N. Tran, C. O. Plamondon, L. Tuduri, D-V. N. Vo, S. Nanda, A. Mishra, H-P. Chao, A. K. Bajpai, *Prog. Org. Coat.*, 2019, **132**, 235-256.
[206] P. Nguyen-Tri, T. A. Nguyen, P. Carriere, C. Ngo Xuan, *Int. J. Corros.* 2018, **2018**, 1–19.
[207] R. Asmatulu, M. Ceylan, N. Nuraje, *Langmuir*, 2011, **27(2)**, 504–507.
[208] M. Long, S. Peng, W. Deng, X. Yang, K. Miao, N. Wen, X. Miao, W. Deng, *J. Colloid Interface Sci.,* 2017, **508**, 18–27.
[209] P. Kim, T. J. Kang, *Micro Nano Sys. Lett.* 2017, **5**, 18.
[210] L. Y. Wang, J. P. Tu, W. X. Chen, Y. C. Wang, X. K. Liu, C. Olk, D. H. Cheng, X. B. Zhang, *Wear*, 2003, **254 (12)**, 1289–1293.
[211] N. Zhang, Y. Zhang, Y. J. Xu, *Nanoscale* 2012, **4**, 5792–5813.
[212] M. Panahi-Sarmad, B. Zahiri, M. Noroozi, *Sens. Actuator A-Phys.* 2019, **293**, 222-241.
[213] N. J. Kanu, E. Gupta, U. K. Vates, G. K. Singh, *Compos. Part A Appl. Sci. Manuf.,* 2019, **121**, 474-486.
[214] P. Majumdar, D. C. Webster, *Macromolecules,* 2005, **38**, 5857-5859.
[215] P. Majumdar, S. Stafslien, J. Daniels, D. C. Webster, *J. Coat. Technol. Res.*, 2007, **4 (2)**, 131-138.
[216] A. Ekin, D. Webster, J. Daniels, S. Stafslien, F. Casse, J. Callow, M. Callow, *J. Coat. Technol. Res.,* 2007, **4 (4)**, 435-451.
[217] G. Wang, D. Yu, A. D. Kelkar, L. Zhang, *Prog. Polym. Sci.,* 2017, **75**, 73-107.
[218] S. K. Rath, J. G. Chavan, S. Sasane, A. Srivastava, M. Patri, A. B. Samui, B. C. Chakraborty, S. N. Sawant, *Prog. Org. Coat.* 2009, **65 (3)**, 366-374.
[219] A. Steele, I. Bayer, E. Loth, *Nano Lett.,* 2009, **9(1)**, 501–505.
[220] Q. W. Xu, C. A. Barrios, T. Cutright, B. M. Z. Newby, *Environ. Sci. Pollut. Res.,* 2005, **12**, 278–284.
[221] E. R. Holm, E. G. Haslbeck, A. A. Horinek, *Biofouling*, 2003, **19(5)**, 297–305.
[222] V. Vatanpour, A. Shockravi, H. Zarrabi, Z. Nikjavan, A. Javadi, *J. Ind. Eng. Chem.*, 2015, **30**, 342-352.
[223] H. Wu, B. Tang, P. Wu, *J. Memb. Sci.*, 2014, **451**, 94–102.
[224] M. Safarpour, V. Vatanpour, A. Khataee, Desalination, 2016, **393**, 65-78.
[225] M. Safarpour, A. Khataee, V. Vatanpour, *J. Memb. Sci.*, 2015, **489**, 43–54.
[226] B. Li, T. Liu, Y. Wang, Z. Wang, *J. Colloid Interface Sci.*, 2012, **377**, 114–121.
[227] B. J. Hong, O. C. Compton, Z. An, I. Eryazici, S. T. Nguyen, *ACS Nano* 2012, **6 (1)**, 63–73.
[228] S. Deng, V. Tjoa, H.M. Fan, H.R. Tan, D.C. Sayle, M. Olivo, S. Mhaisalkar, J. Wei, C.H. Sow, J. Am. Chem. *Soc.*, 2012, **134**, 4905−4917.
[229] J. Wang, T. Tsuzuki, B. Tang, X. Hou, L. Sun, X. Wang, *ACS Appl. Mater. Interfaces*, 2012, **4 (6)**, 3084-3090.
[230] T. Shen, D. Lang, F. Cheng, Q. Xiang, *Chem. Select.*, 2016, **5**, 1006–1015.
[231] L. Sun, T. Du, C. Hu, J. Chen, J. Lu, Z. Lu, H. Han, *ACS Sustainable Chem. Eng.,* 2017, **5(10)**, 8693–8701.
[232] J. F. Schumacher, N. Aldred, M. E. Callow, J. A. Finlay, J. A. Callow, A. S. Clare, A. B. Brennan, *Biofouling*, 2007, **23**, 307–317.
[233] K. Ellinas, A. Tserepi, E. Gogolides, *Adv. Coll. Interface Sci.,* 2017, **250**, 132-157.
[234] Y. Y. Yan, N. Gao, W. Barthlott, *Adv. Coll. Interface Sci.,* 2011, **169 (2)**, 80-105.
[235] S. Krishnan, N. Wang, C. K. Ober, J. A. Finlay, M. E. Callow, J. A. Callow, A. Hexemer, K. E. Sohn, E. J. Kramer, D. A. Fischer, *Biomacromol.,* 2006, **7**, 1449–1462.
[236] D. McMaster, S. Bennett, Y. Tang, J. Finlay, G. Kowalke, B. Nedved, F. V. Bright, M. E. Callow, J. A. Callow, D. E. Wendt, M. G. Hadfield, M. R. Detty, *Biofouling*, 2009, **25**, 21–33.
[237] M. M. Rahman, H. H. Chun, H. Park, *Macromol. Res.*, 2011, **19**, 8–13.
[238] R. Akid, H. Wang, T.J. Smith, D. Greenfield, J.C. Earthman, *Adv. Funct. Mater.*, 2008, **18**, 203–211.

Table 1. A wide-range survey of fouling-prevention methods and antifouling advances

Timeline	Description of antifouling product	Reference
Oldest	Tar, asphalt, and wax	60
700 B.C.	Carthaginians & Phoenicians used pitch, sheathing with copper and lead, and tallow	1, 60
500 B.C.	Phoenicians developed Arsenic and sulphur in oil coatings	1, 59
300 B.C. – 45	Greeks & Romans used Tar, wax, and sheeting with lead with nails of copper	68
10	Seal tar was used by Vikings	59, 60
45–125	Plutarch used pitch, algae scrapings	59
1300-1500	Pitch mixed with oils, Pitch and tallow were used by Columbus's vessel	59,60
1618-1625	Arsenic ore, copper, and iron dust	59
1625	1st Coating patent by William Beale	59
18th century	Wood sheathing on a pitch layer, pitch, fat,	1
1758 A.D.	Copper sheathing by the English (Frigate HMS Alarm)	60
	Copper sheathing with Zinc alloy	60
	Iron Ships	
1800-1900s	Sir Humphrey Davy reported that copper dissolution in sea water prevented fouling. So, copper, arsenic, and mercury were incorporated into coatings	1, 59
1847	Application of insulating primer under the antifouling layer	60
1860	Hot plastic paints (metallic soap composition such as copper sulphate)	1
1863	Antifouling paint by using tar	59,60
Late 19th century	Shellac primer and shellac antifouling coating with different toxicants	1, 60
1926	Cold plastic paints including coal tar + colophony and synthetic resins	60
1950-1960	Development of the first organometallic paints (tri-organotins $(R)_3$-Sn in acrylic ester-based coatings	1
1976	TBT-SPC technology, 1976 patent, allowed control of biocide release rates	1, 59, 68
1977	First FR coating patent	1
1980s	- Development of TBT-SPC coatings allowed control of biocide release rates. - TBT linked to shell abnormalities in oysters and imposex in dog whelks.	1, 59
1987-1990	TBT coatings prohibited on vessels	1,59
1990s	Copper release rate restrictions introduced in Denmark and considered elsewhere e.g. California, USA	1, 60
2000s	Research into environmentally friendly AF alternatives increases	59
2001	International Maritime Organization (IMO) adopts''AFS Convention'' to eliminate TBT from AF coatings from vessels through: 2003 – prohibition of further application of TBT. 2008 – prohibition of active TBT presence.	60
2001	FR coatings based on silicone and fluoropolymer matrixes	1
2002	A group designed engineered PDMS-based microtopographies composed of pillars or ridges with various heights.	61
2004	Lotus leaf structure has been studied in detail by Marmur showed two-dimensional roughness in leaf appendixes of several micrometres in size and covered with nano-micro sized wax crystals	62
2006	Carman et al. demonstrated a bioinspired surface, Sharklet AF™	63
2009	Chung and others demonstrated that the Sharklet AF™ topography inhibited biofilm formation of Staphylococcus aureus over a period of 21 days.	64
Since 2009	The change in wettability of a surface due to micro-topographical roughness is also likely to be a contributing factor to antifouling properties.	65
2011	Superhydrophobic surface based on silica colloids and a low surface energy fluorinated silane xerogel reduced the fouling adhesion	66
2010-2018	Development of inorganic-organic hybrid nanocomposite for self-cleaning and FR coatings (Different nanofillers, polymers and silicone copolymers) were used.	4, 22, 67, 122
2017-2019	Various series of silicone homo(co)polymer/hybrid nanofiller composites as a self-cleaning and FR coatings termed as ternary and quaternary nanocomposites	1, 4, 9, 22

Table 2: Different techniques used for developing of superhydrophobic antifouling nanocomposites

Technique	Describtion	Merits	Limitations	References
In-situ polymerization	This technique allows dispersion of nanofiller into the monomer of the polymer matrix used. Polymerization reaction is facilitated by the incorporation of initiator or thermal and photocatalyst.	* High level of nanofiller distribution into matrix compared to other techniques. * Free of contaminations. * Suitable for insoluble polymers. * High miscibility.	* Difficulty in intergallary polymerization. * High cost. * Small scale.	197, 199
Solution casting technique	Nanofiller was ultra-sonicated in a suitable solvent before adding to the polymer matrix. Then, the solvent was removed by evaporation at room temperature or by heating, followed by washing the fabricated composite film and further dried.	* Simple and common method to homogenously-distributed nanocomposites. * This method was utilized to incorporate many nanofillers in different polymeric matrixes.	* The used solvent should be removed by evaporation. * Low dispersion is achieved than in situ method.	200
Melt intercalation	No processing solvent is required; however dispersion takes place directly in the molten state of thermoplastic polymer via conventional techniques like injection molding and extrusion. The polymer was melted and powder filler was mixed under high shear conditions in the mixing approach.	* An economic method (i.e., as no solvent is used). *High matrix-nanofiller compatibility.	* Low dispersion ability of nanofillers in the polymer matrix.	201
Sol-gel	In a typical sol–gel process, the precursor is converted into a glassy material through a series of hydrolysis and poly-condensation reactions. By varying the system conditions and reaction mixtures, the surface roughness can be controlled.	* Complex surfaces. * High quality films. * Good resistance to temperature.	* Crackability. * Thickness limits.	202, 203
Chemical vapor deposition	In the deposition process, the chemical precursors are transported in the vapor phase to decompose or react on a heated substrate to form a film. CVD can be applied whether to create rough surfaces or to depose a thin layer of hydrophobic compound on a rough surface.	* High quality coatings. * Thickness controllable. * Complex surface.	* High temperature. * High cost.	154–149, 204
Dip-coating	It is usually consisted of two steps: (1) the soaking of a substrate in a solution containing nanoparticles and it's upwards pulling at a constant and controlled speed; (2) the substrates are then covered by a water repellent agent after its removal from the solution. Due to the imposed pull-up rates, the nanocoating thickness on the substrate surface is also controlled.	* Complex surface. * Industrial scale. * Materials reusable.	* Large amount of solvent. * Only for soluble polymers.	205, 206
Electro-spinning	Nanofiller materials were ultra-sonicated in DMF solvent and the mixture was dissolved in the polymeric resin to prepare the precursor fiber composite mixture. A syringe was used to electro spun the prepared composite mixture at 5-20 kV positive voltage. The high voltage used provides a charged liquid surface and facilitates the electro-spinning of the composite mixture.	* High quality coating. * High-voltage application can form ultra-fine micro- and nano composite fibers which are electrospun by solvent evaporation. * Quick drying.	* To control the polymer properties (i.e., form, molecular weight and viscosity), the utilized solvent, voltage used, and the distance between the needle and the substrate should be monitored. * Small surface. * Laboratory scale.	207, 208
Electro-deposition	A facile technique was used to synthesis graphene-based nanocomposites via electrochemical methods. A working electrode (electrically conductive surface was used to deposit the nanofibers layer) and reference and platinum counter electrodes were included in the electro-deposition cell. The formed nanofibers produced by electro-deposition method are filmed on the conductive working electrode.	* High quality coatings. * Low cost. * Simple manufacturing process.	* Environmental issues. * Time consuming. * Non-uniform coating.	209, 210

Table 3. Recent development of non-biocidal antifouling coatings and their building blocks designs

Antifouling/fouling release coating type	Antifouling/fouling release testing against:	Stage of development	References
Sharklet AF™ PDMSe	Balanus improvisus cyprids, Amphora (diatom), Ulva rigida (green algae), Centroceras clavulatum (red algae), Hydroides elegans (tubeworm) and Bugula neritina Linneaus (bryozoan).	Research	232
Fouling release --Fluorinated polymers and silicon	Barnacles, Ulva, Navicula, polychaetes, bryozoans.	Commercially-available	233
Sol–gel coatings	Protein (BSA) and a variety of fouling organisms including juvenile barnacles (Balanus amphitrite), oysters, polycheates, algae, Ulva marine biofouling.	Research	234, 235
Fluorinated and PEGylated stripe patterns	Ulva-zoospore settlement	Research	236, 237
Block copolymer containing fluorine in which the Ag-loaded mesoporous silica (Ag@SBA) is embedded	Pseudomonas fluorescens was carried out in the agar plating	Research	238
The incorporation of only 0.5% ZnO-SiO_2 nanospheres minimized the surface tension and improved fouling resistance	Some models of biological foulant for biofilm formation such as bacteria (Micrococcus sp. and Pseudomonas putida) and fungi (Aspergillus niger) have been investigated.	Research	108

Journal Name

ARTICLE

Figures:

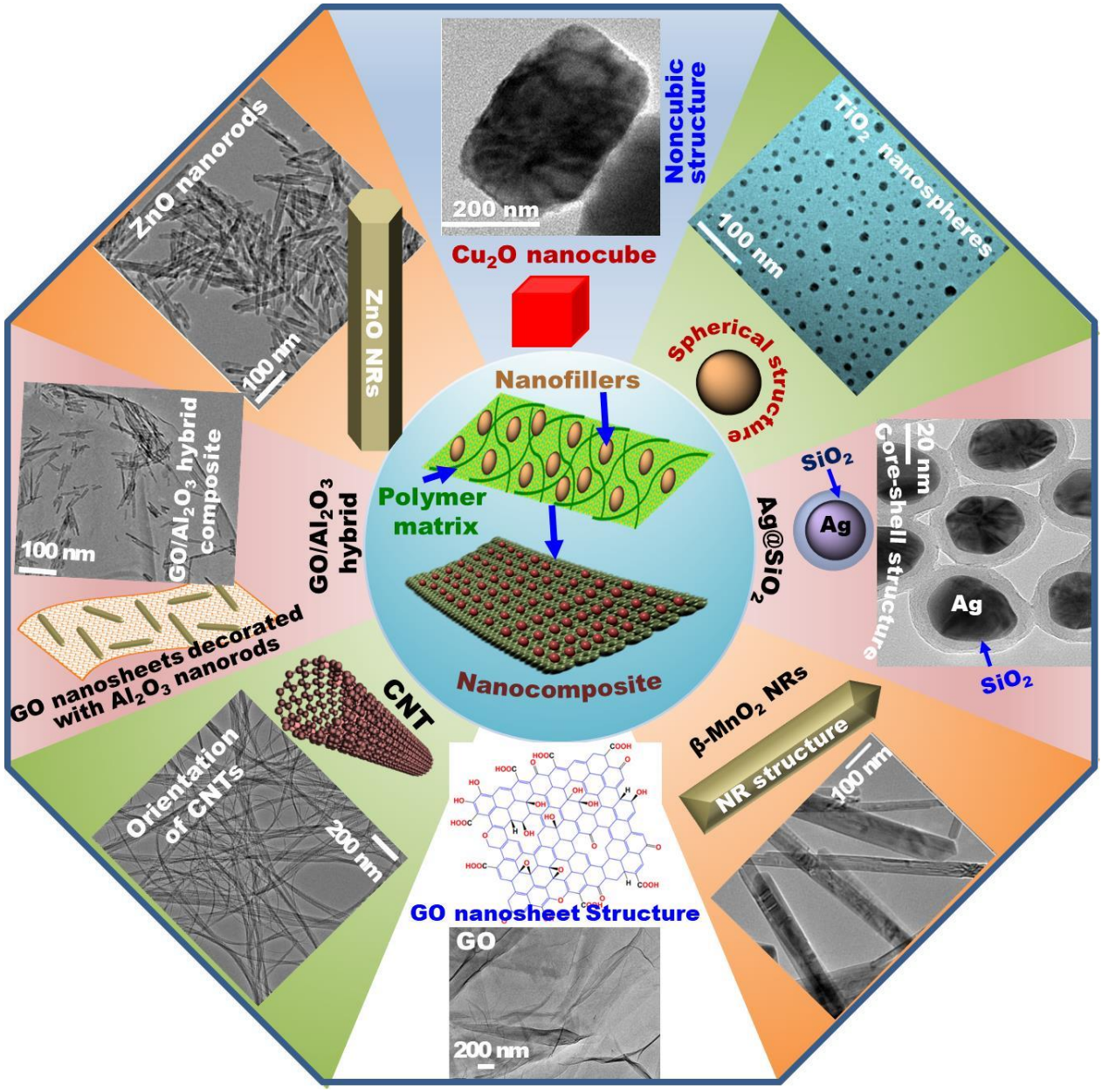

Figure 1. Schematic illustration of design components of self-cleaning nanocomposites as follows: Outer images represented the microscopic patterns (i.e., transmission electron microscope, TEM) for nanofiller materials with different nanoscale orientations, configurations, arrangements, and directions (middle-centre) associated with the fabricated architectural composite building-blocks (core centre). The nanofiller included Cu_2O nanocubes, TiO_2 nanospheres, Ag@SiO_2 core-shell, β-MnO_2 nanorods, GO nanosheets, CNTs, GO/Al_2O_3 hybrid, ZnO nanorods.[26] These nanofillers-hybrid polymeric matrixes lead to design self-cleaning nanocomposites for marine antifouling coatings.[1,26] Copyright 2019, reproduced after permission from Elsevier publisher.

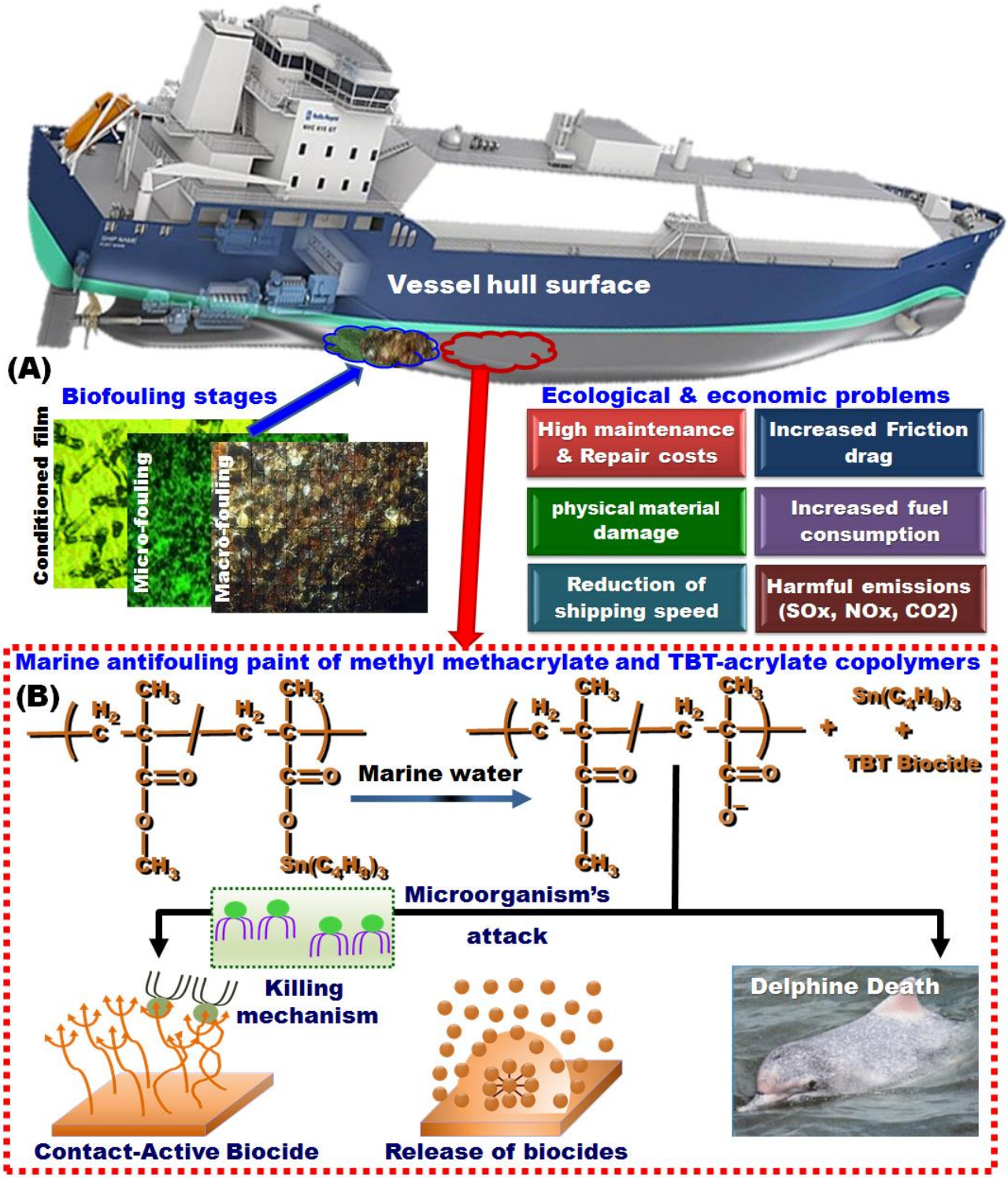

Figure 2. (A) Representative scheme for biofouling stages including biofilm, microfouling, and macrofouling; which were caused by the adhesion of fouling organisms on the marine ship hulls.[1,39] (Bottom) Illustration of the severe ecological and economic problems as well as the physical and maintenance disastrous caused by the adhesion of fouling organisms on the ship hulls.[1,45] Copyright 2018, reproduced after permission from Elsevier. (B) Illustration of the biocide-release mechanism of methyl methacrylate and TBT-acrylate copolymers as a marine antifouling paint, which prohibits the biofouling through biocidal influences.[43] The polymeric resin is decomposed during hydrolysis of the copolymer units in the marine water. The release of TBT-based biocides can kill not only fouling organisms but also non-target species such as dolphins and fishes (right-side).[1,43] Biocidal antifouling coatings caused marine environmental pollution and economic losses. Copyright 2017, reproduced after permission from Elsevier.

Figure 3. Examples of superhydrophobic self-cleaning surfaces in the natural plants and animals; where (a) represents an image of the superhydrophobicity of the surfaces of lotus leaves; (b) Water drop in its spherical shape over the lotus surface; (c) SEM captures of lotus leaves at high magnification power; this surface has water-repellent epicuticular waxy architecture formed with 20–40 μm protruding ganglion.[26,80] (d) Rice-effect which is hybrid between lotus-effect and shark-skin effect. The drops of water are staying over low free energy and hydrophobic surface, and (e) the leaves of rice plant with grooves and sinusoidal pattern.[80] (d) Wings of butterflies; (e) SEM image of the wings of butterflies with directional adhesion having radial outward direction; thus exhibit superhydrophobic self-cleaning, (f) Legs of water striders on the surface of water, (g) Macrosetae with needle-like shape and grooved structure on the surface of strider leg.[80] Copyright 2011, Adopted after the permission from Elsevier. (j) Indicates biofouling on the Humpback whale skin, high magnification images indicated that its skin is covered with barnacles, while (k) illustrates a self-cleaning skin of a Mako shark. SEM capture for the shark surface shows fine tooth-shaped dermal surfaces that have longitudinal grooves with ribbed structures; thus, the skin of Mako shark provide reduced resistance against fouling organisms.[94] Copyright 2014, Adopted after the permission from Elsevier.

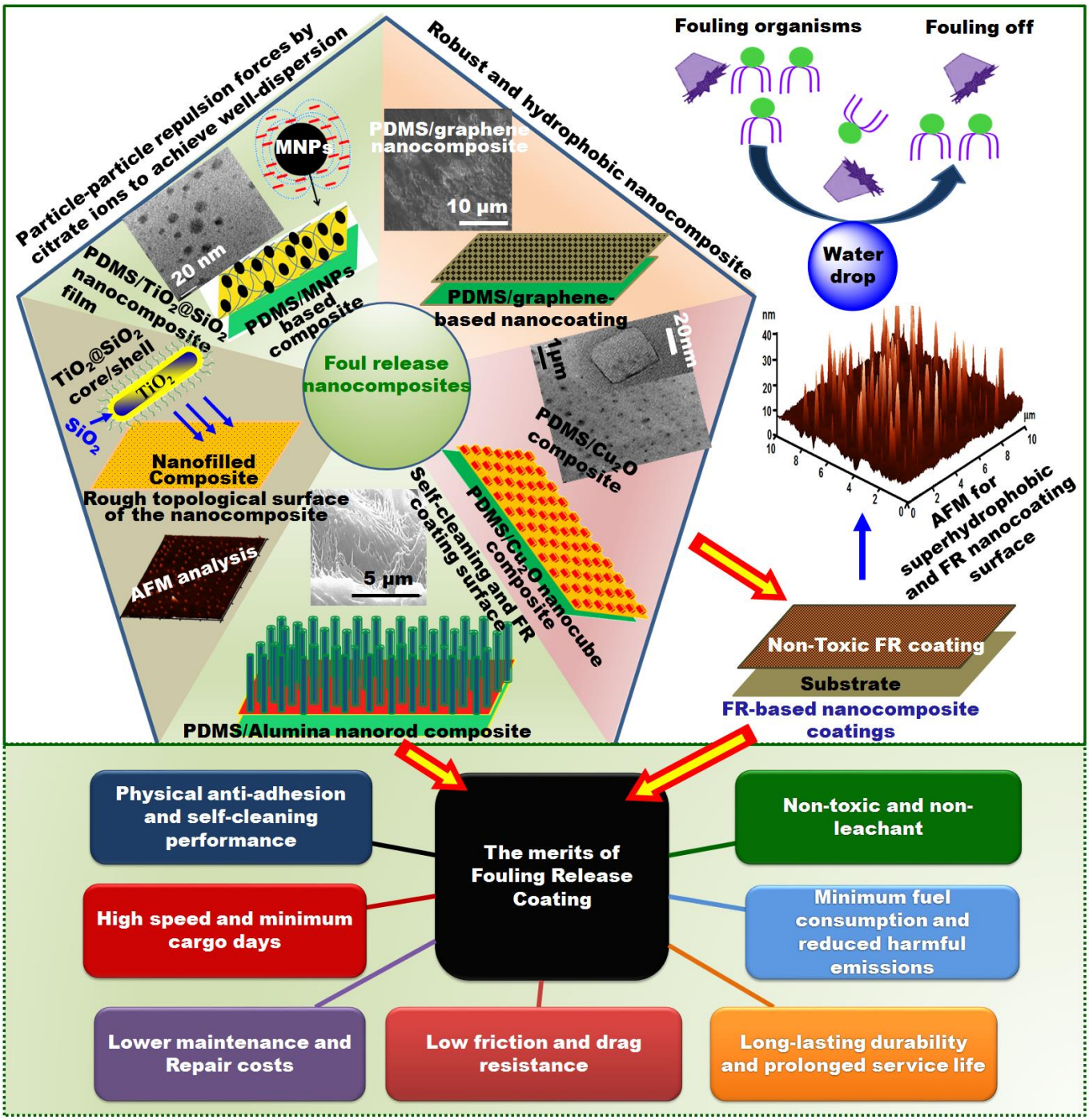

Figure 4. Schematic illustration (as well as SEM, TEM, and AFM) of developed silicone filled nanocomposites for FR coating applications. The physical antiadhesion mechanism was illustrated that can prevent fouling settlements without toxicity. The environmental and economic merits of fouling release coating nanocomposite surfaces. These non-toxic surfaces provide efficient solutions for biofouling problem in the marine environments and internationally accepted alternative for the toxic antifouling paints.[26,98,109]

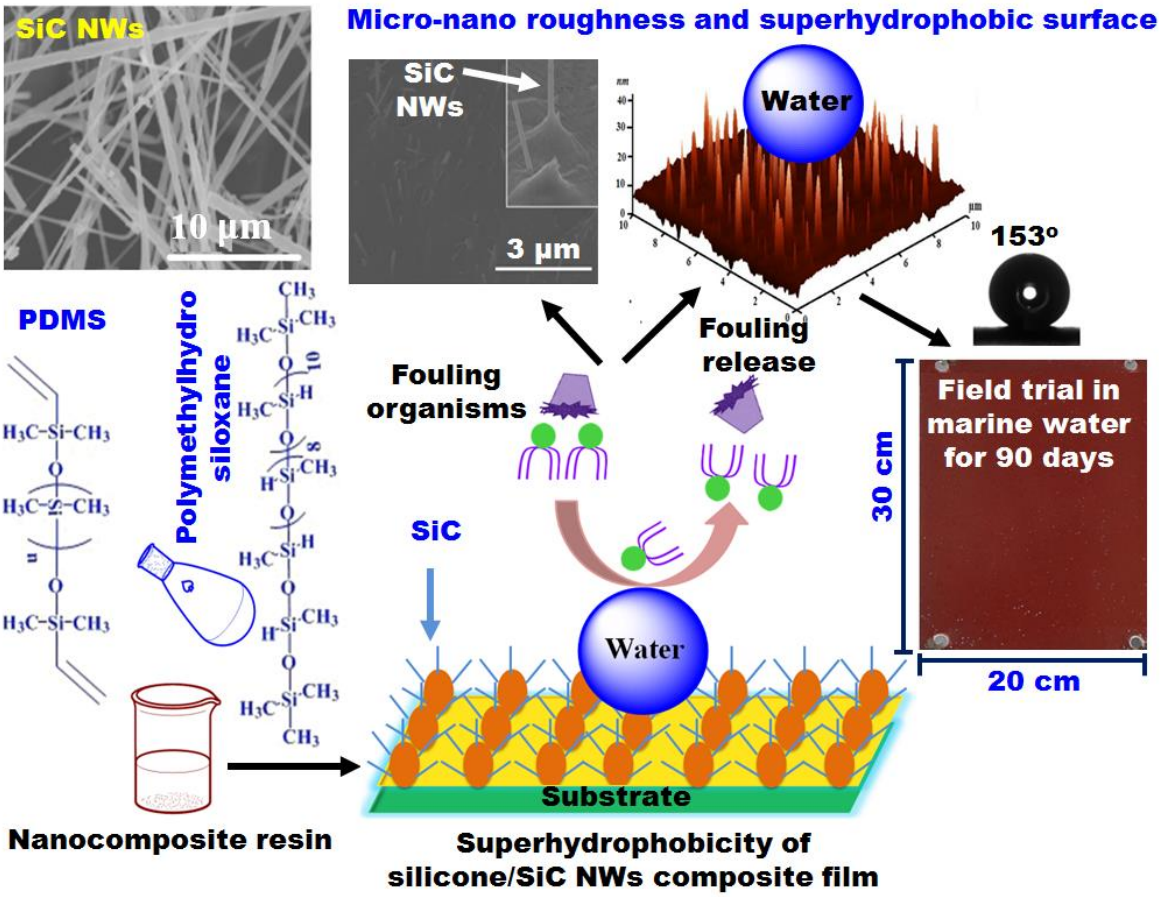

Figure 5. Applying a composite of silicone/SiC NWs through ex situ method as a self-cleaning and FR surface. The nanocomposite was cured via hydrosilation curing technique. Inside the SEM of SiC NWs as well as SEM and three-dimensional AFM of PDMS/SiC NWs composite with its micro/nanorough surface that cause fouling release. A Field test was carried out for the developed nanocomposite through immersion in natural water for 90 days; which illustrated high resistance against fouling adhesion.[9] Copyright 2018, adopted after permission from Springer Nature.

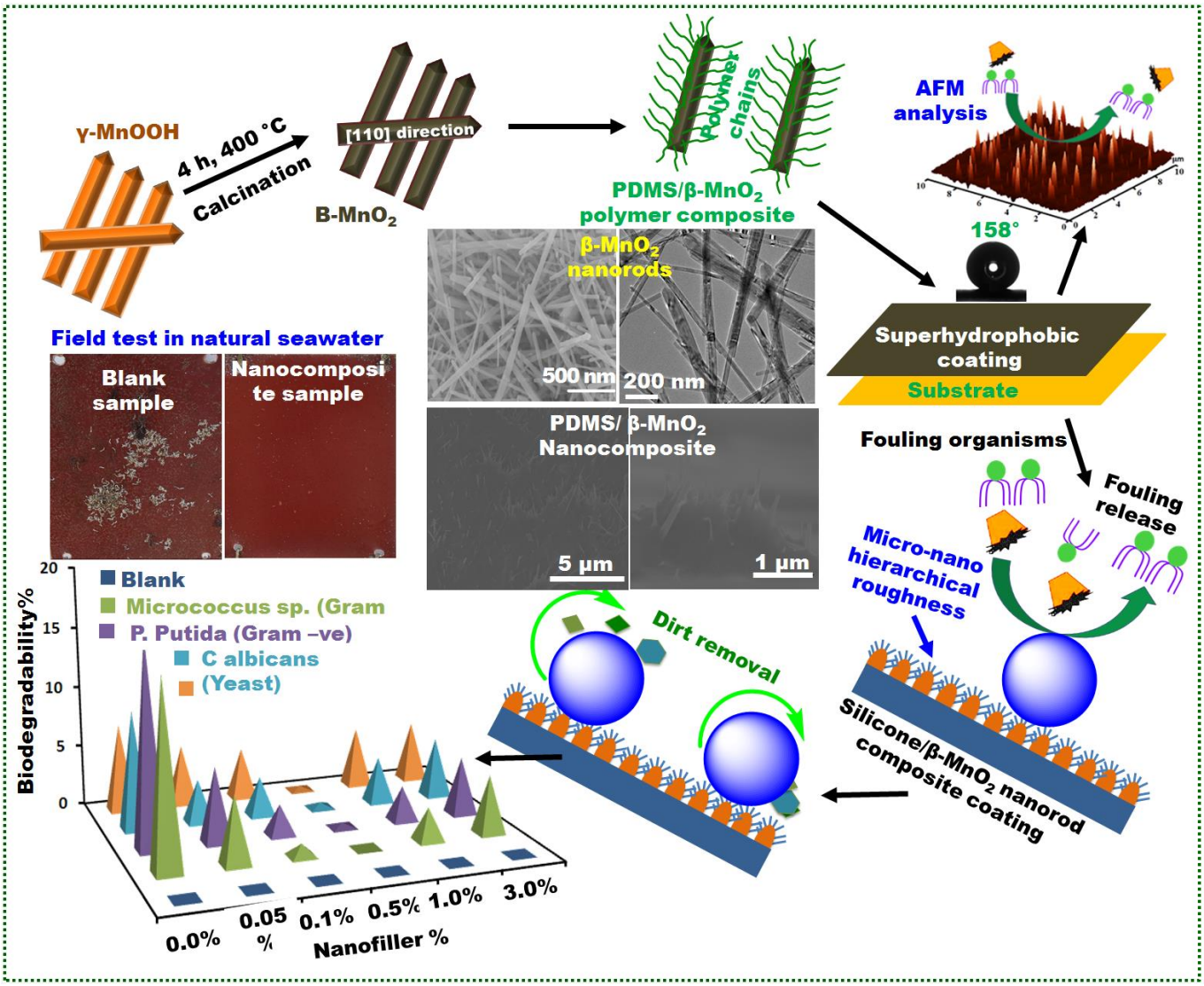

Figure 6. Illustration of the controlled-synthesis process carried out through hydrothermal and calcination methods to yield β-MnO_2 nanorods with [110] growth direction; inside the TEM and SEM images of β-MnO_2 nanorods. Also, PDMS/β-MnO_2 nanorod (0.5 wt.%) composite was fabricated through in-situ process to produce self-cleaning and fouling release coatings. AFM and two SEM images (at different magnification powers) were elucidated to indicate the preparation of micro/nano-rough surface. Superhydrophobicity of the nanocomposite and self-cleaning design was illustrated. Biodegradability test was performed on a series of nanocomposites prepared through different nanofiller percentages; where high antifouling effect was reflected for the well-dispersed nanocomposite (0.5 wt.% nanofiller concentration). Comparison of the unfilled sample and the well-dispersed nanocomposite sample was carried out through visual evaluation and an imaging method; which illustrated the high fouling-resistance for the well-dispersed sample.[142] Copyright 2019, reproduced with permission from Elsevier Ltd.

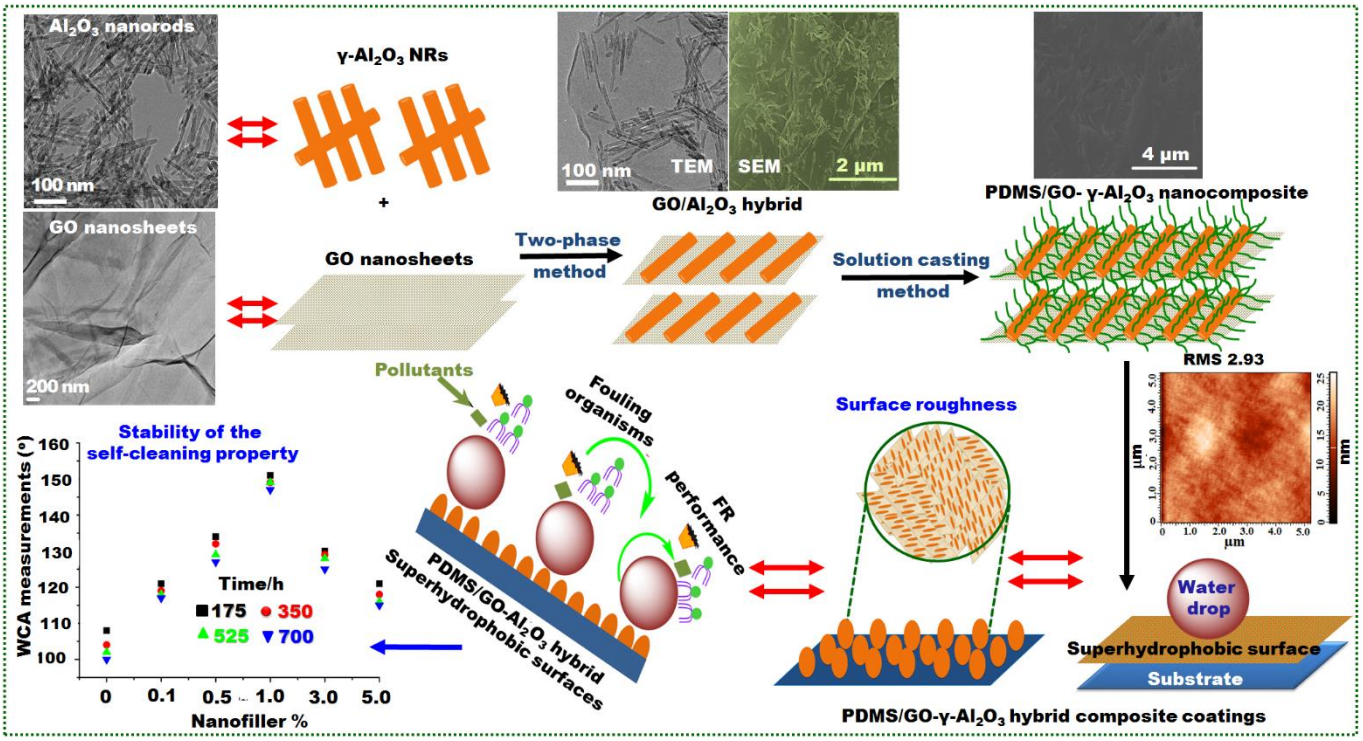

Figure 7. Schematic illustration of the hybridization between GO nanosheets (synthesized through a modified Hummer's method) and γ-Al2O3 (prepared and controlled through hydrothermal and calcination methods) to yield GO/γ-Al_2O_3 hybrid. Inside the TEM images of GO sheets, γ-Al_2O_3 nanorods and GO/γ-Al_2O_3 hybrid were indicated. Designing superhydrophobic PDMS/GO-γ-Al_2O_3 nanorods hybrid composites was carried out through a solution casting method followed by hydrosilation curing to yield self-cleaning and FR coating surface. AFM and SEM of the nanocomposite surface indicated the surface roughness; which was represented in through discussing the FR mechanism. The FR effectiveness is enhanced by well-dispersion of GO/γ-Al_2O_3 hybrid nanofillers. Also, thermal stability of the WCAs of the nanocomposites was compared among a series of nanofiller concentrations and showed the highest effectiveness for well-dispersed (1 wt.%) nanofillers.[146] Copyright 2018, reproduced with permission from Elsevier.

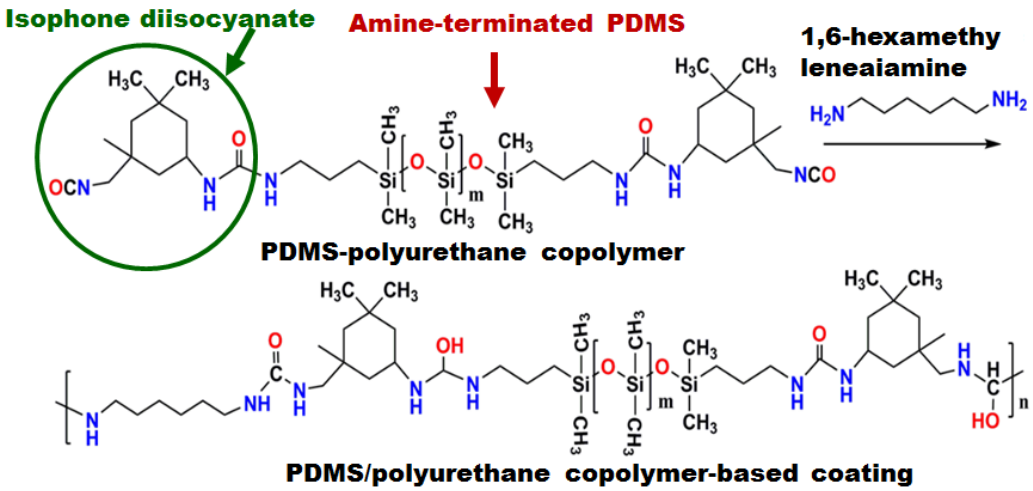

Figure 8. Polydimethylsiloxane-polyurethane block copolymer for marine fouling release coatings; this copolymer can fuse together the self-cleaning and antifouling properties of PDMS with the mechanical robustness of polyurethane.[162]

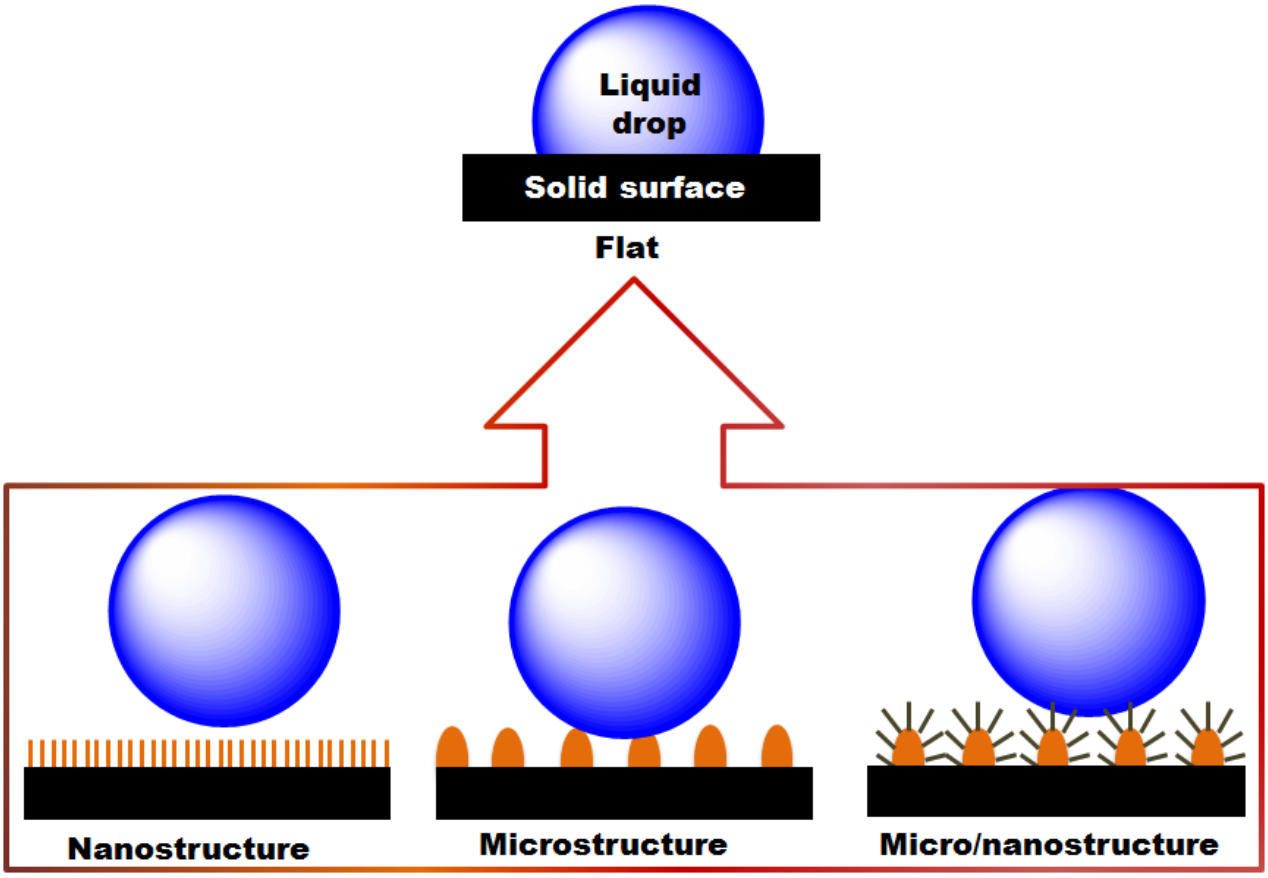

Figure 9. Surface roughness is important factor for enhancing superhydrophobic coating material than the flat solid surface. Roughness designs include nanostructured, micro-structured, and micro/nano-structural surfaces of the prepared nanocomposites; which can prevent fouling through physical anti-adhesion mechanism and provide self-cleaning features.[168]

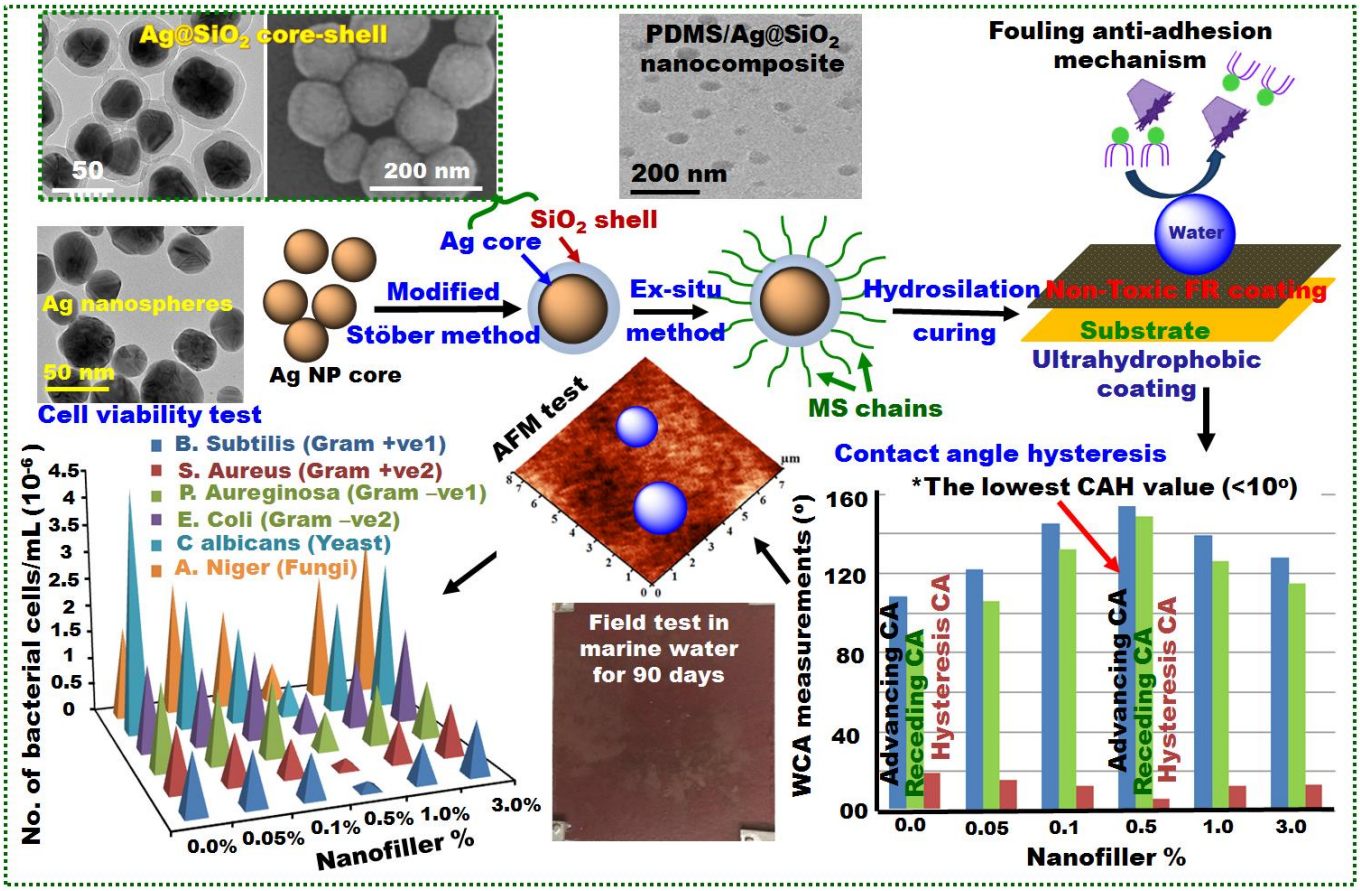

Figure 10. Schematic Illustration of the nanocomposite of PDMS/Ag@SiO_2 nano spherical composites which was reported as efficient FR coating material. The Ag nanospheres, which prepared through High-temperature solvothermal procedure, was shelled by 2-5 nm shell-thickness of SiO_2 via a modified stopper method. PDMS/Ag@SiO_2 nanocomposite was prepared through ex-situ method and cured via a hydrosilation curing mechanism and filmed to form FR coating surface. Different nanofiller concentrations were investigated where the 0.5 wt.% showed the lowest CAH (<10°) and cell viability. The surface topology was investigated through AFM, dispersion of the core shell nanospheres was pictured through TEM image, and the field test was studied through a field test in natural water.[177] Copyright 2018, adopted after the permission from RSC.

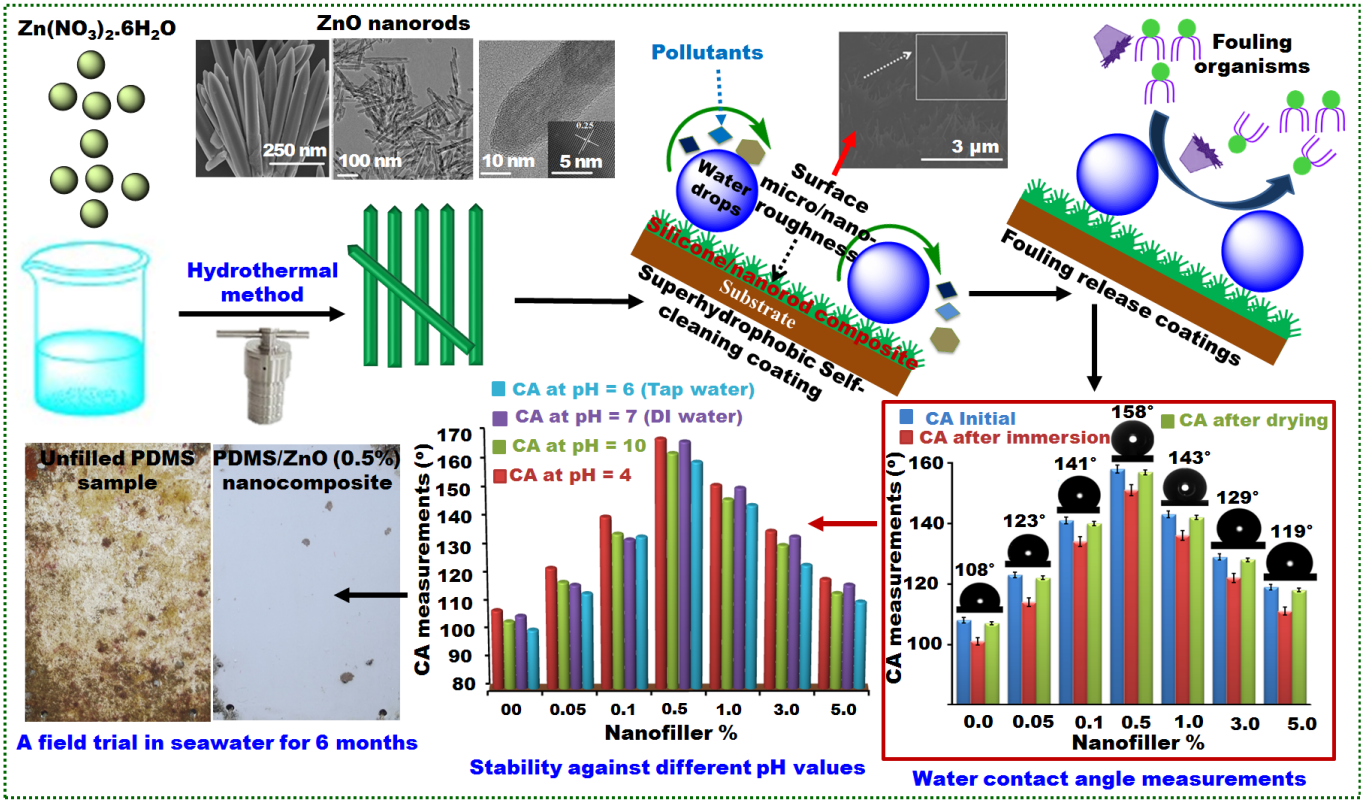

Figure 11. The superhydrophobic, self-cleaning and FR characteristics for PDMS/ZnO nanorod composite surface. A wet-chemical method followed by calcination were used top ZnO nanorods; inset the SEM, TEM (at different magnifications), and crystal lattice of the nanorods. While, in-situ fabrication method is used for preparing PDMS filled with ZnO nanorods composites using different ZnO nanorod concentrations. The nanocomposite was cured and filmed over steel surface to form superhydrophobic micro/nano-roughness topology resemble the lotus like structure as illustrated in the SEM of nanocomposite. Results showed an increase in the static water contact angle with nanofiller loadings up to 0.5 wt.% because of the well-dispersion. Stability of the WCA of the well-distributed nanofillers was also confirmed and reflected the surface renewability. A field experiments showed the high FR effectiveness of the PDMS/ZnO (0.5 wt.%) composite as compared with the unfilled PDMS sample.[180] Copyright 2019, adopted after permission from Elsevier Ltd.

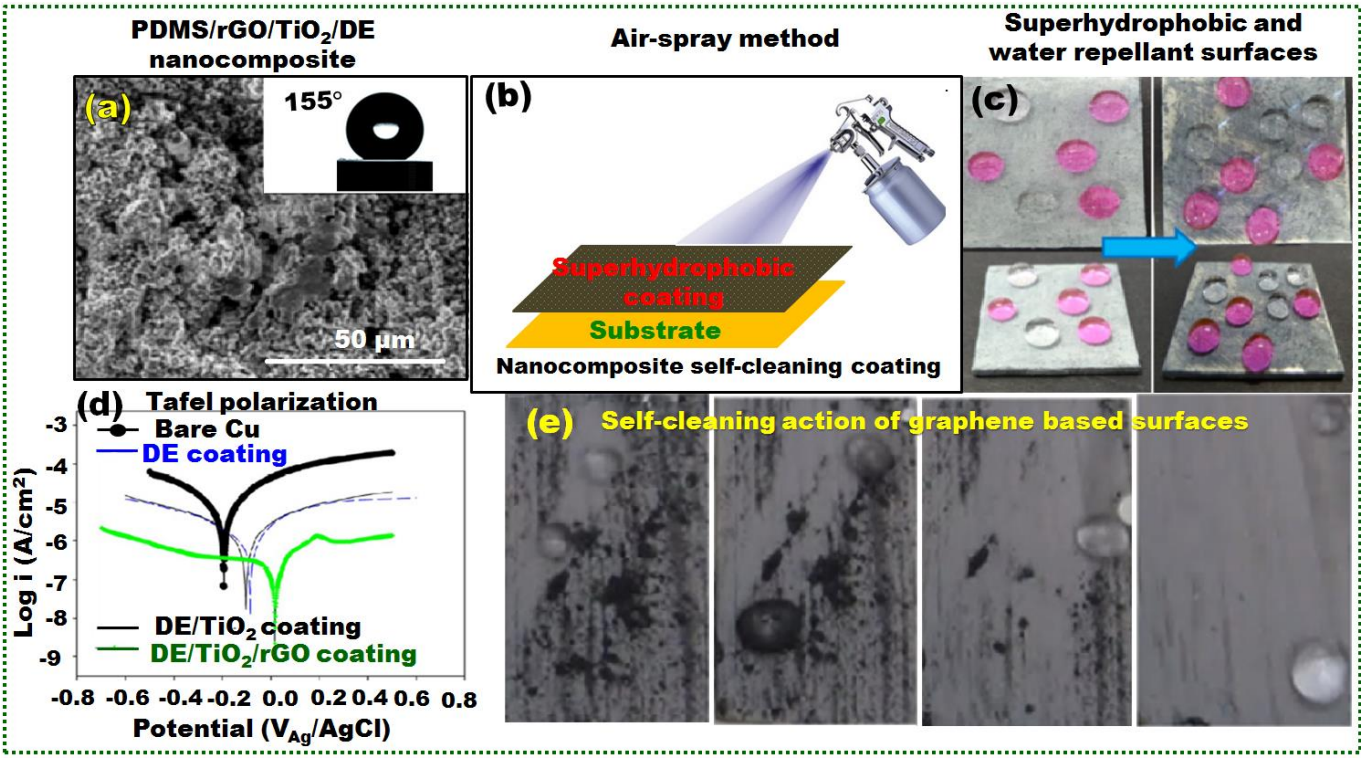

Figure 12. (a) SEM capture for PDMS enriched rGO/TiO_2/DE to yield superhydrophobicity with a WCA of 155°; (b) A schematic representation of nanocomposite surface coated by spray gun over a steel substrate; (c) Ultrahydrophobic action next to sandpaper scratching and abrasion testing for PDMS-coated DE/TiO_2/rGO coating filmed with superhydrophobic property; (d) Curves for Tafel polarization (Electrochemical corrosion test) for virgin rGO/TiO_2/DE as compared with bare Cu and DE, TiO_2, while (e) Self-cleaning action of PDMS coated rGO/TiO_2/DE on the surface of graphitic particles. Copyright 2015, adopted after permission from ACS.[192] Copyright 2015, adopted after permission from ACS.

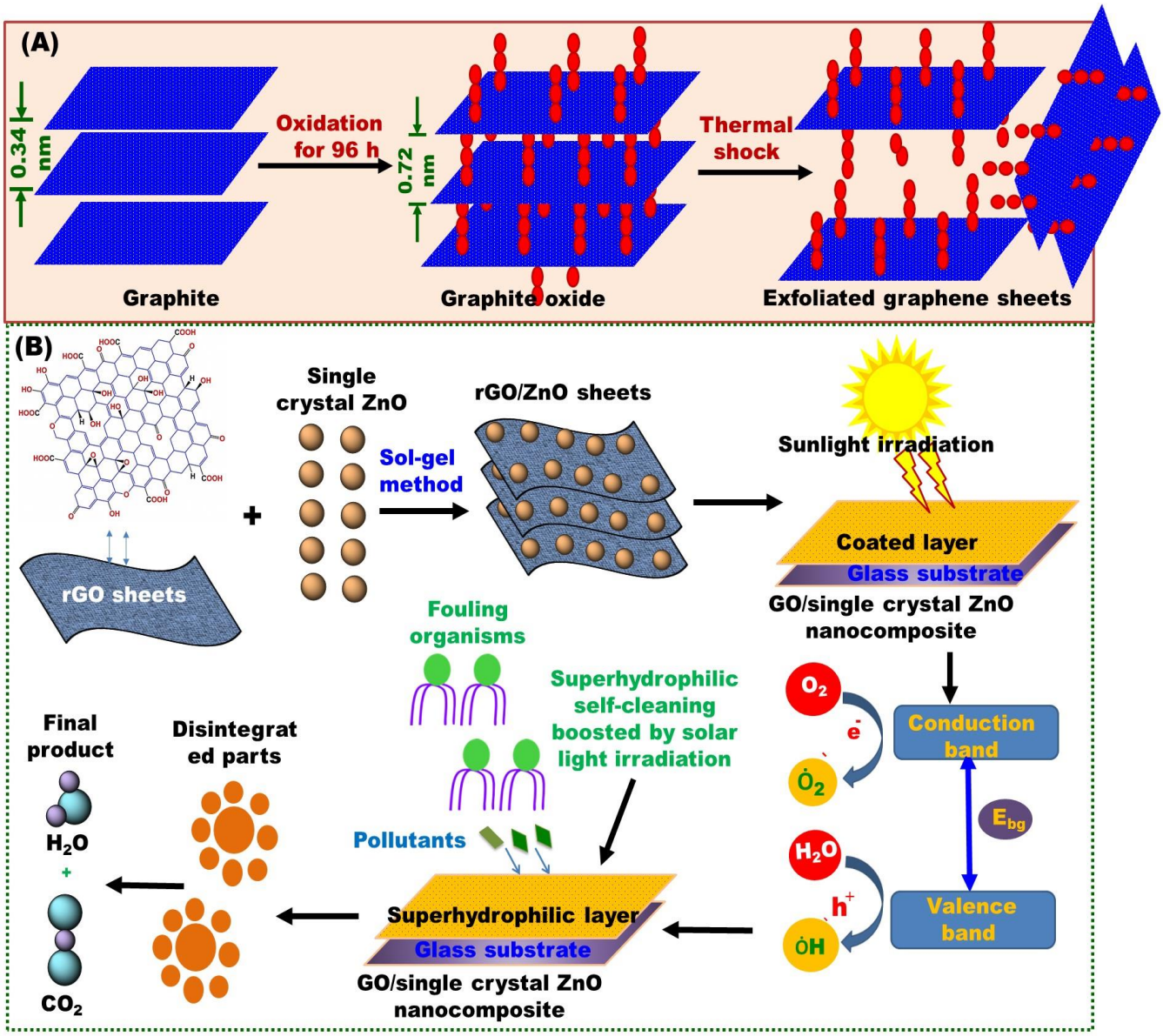

Figure 13. (A) Schematic illustration of exfoliation procedure through oxidation and thermal treatment to yield nanosheets of graphene from graphite powder. The rapid extension of exfoliated GO through intercalation with H_2SO_4 was carried out at 100 °C and R.T.[195] Copyright 2010, adopted after permission from Springer Nature. (B) Solar light boosted FR mechanism proposed for self-cleaning nanocomposite films enriched with (RGO decorated with TiO_2 hybrid) for maritime navigation as reported ealier.[196] A single-phase method can be used to decorate the rGO nanosheets with ZnO nanospheres. This hybrid is filmed over a glass substrate and its photocatalytic self-cleaning is enhanced by UV-Vis irradiation to produce pollutant-repellant and FR nano-surface. The dirt's can be destroyed by solar light to disintegrated parts and finally to CO_2 and H_2O.[1,196] Copyright 2015, adopted after permission from Elsevier Ltd.

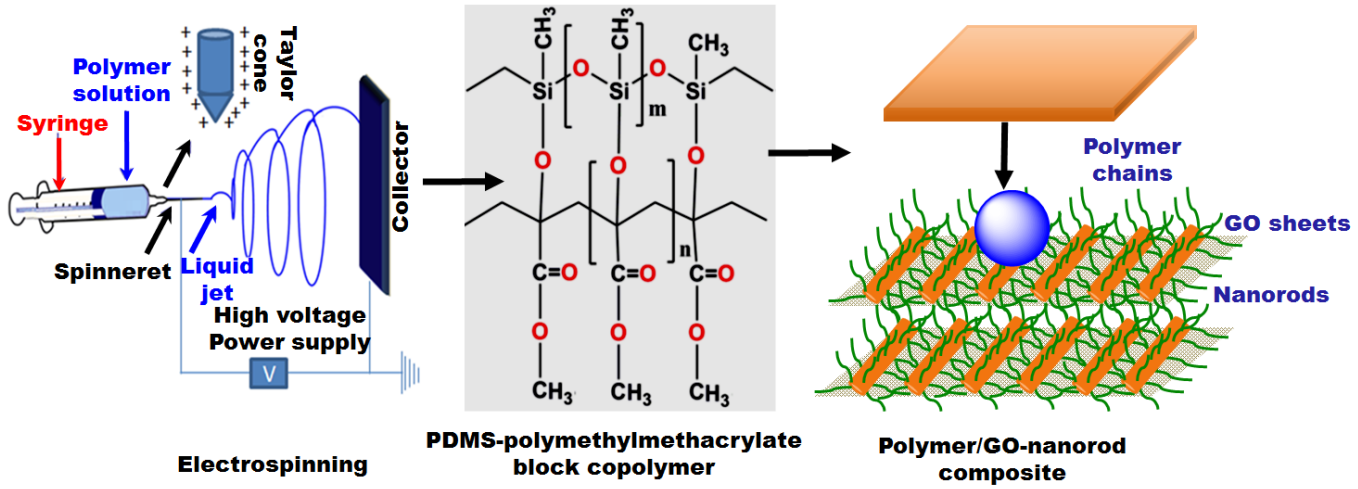

Figure 14. Synthesis and electro-spinning of silicone-polymethyl methacrylate block copolymer. Copolymerization between PDMS and polymethylmethacrylate can fuse together the self-cleaning and mechanical robustness of the surface. This copolymer can be filled with graphene-based nanomaterials for enhancing the FR and mechanical features.[214]

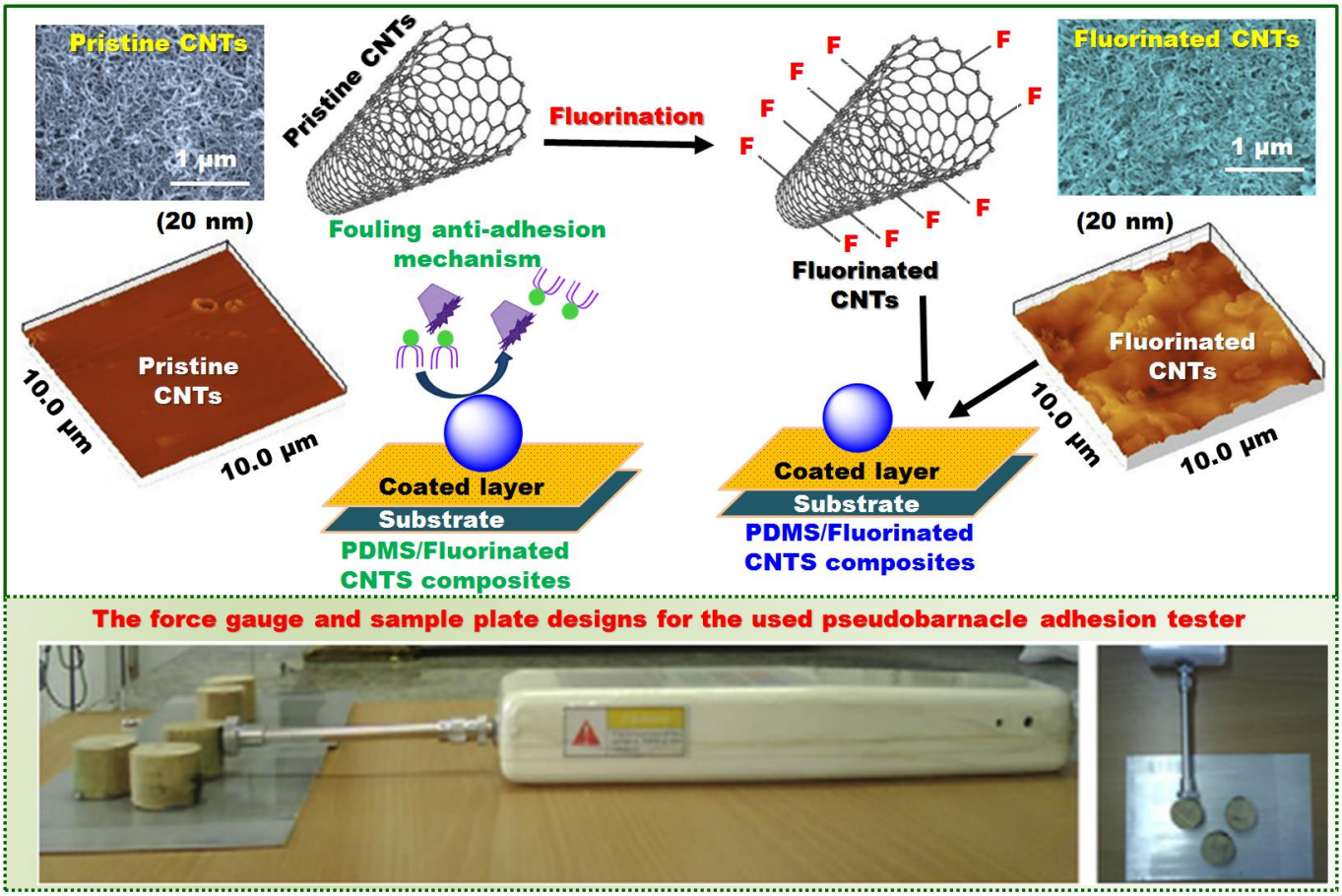

Figure 15. Fluorination of CNTs as a step to prepare fluorinated silicone coatings; the SEM of pristine CNTs and fluorinated CNTs were also illustrated. Fluorinated silicone nanocomposite is a hybrid material that can exhibit enhanced FR and surface self-cleaning properties with more surface for the fluorinated CNTs-based coating as indicated through the AFM analysis. The pseudo-barnacle adhesion test was used to study the FR efficiency and reflected. The fluorinated CNT-enriched PDMS nanocomposite exhibited 67% reduction in the pseudo-barnacle adhesion than the unfilled sample.[164] Copyright 2013, adopted after permission from Elsevier.

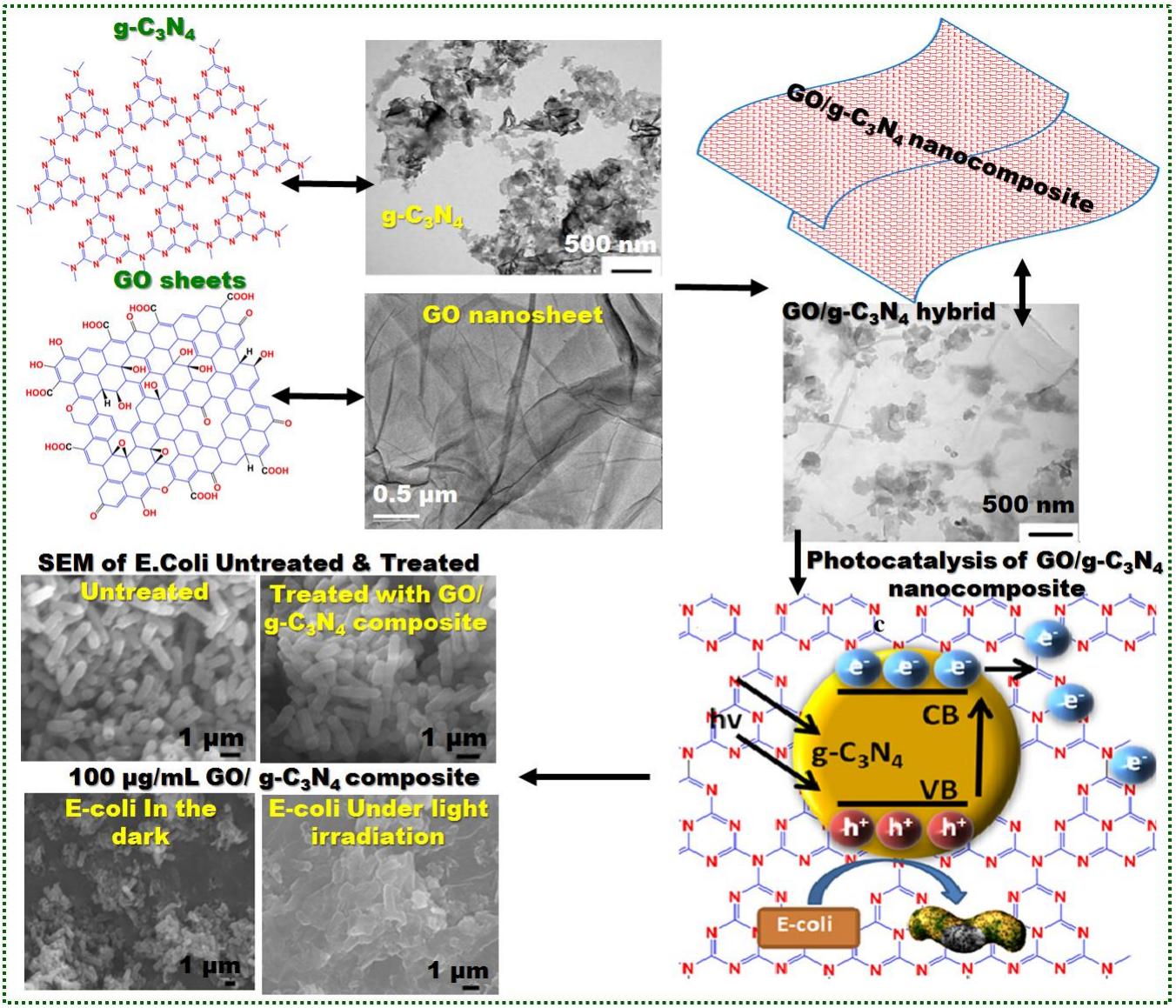

Figure 16. Schematic illustrations of GO/g-C_3N_4 hybrids composite (was developed via ultra-sonication at RT) for applying as antimicrobial agent. TEM images for the products were indicated. High photocatalytic properties and high antibacterial features of the GO/g-C_3N_4 hybrid were presented when testing using E-coli. SEM images of the untreated and treated (in dark and under light) bacterial strains containing 100 μg/mL of GO/g-C_3N_4 was highlighted the high antibacterial performance of the nanocomposite; where 97.9% (E-coli strains) were killed after two-hours of visible irradiation.[231] Copyright 2017, adopted after permission from the American Chemical Society.

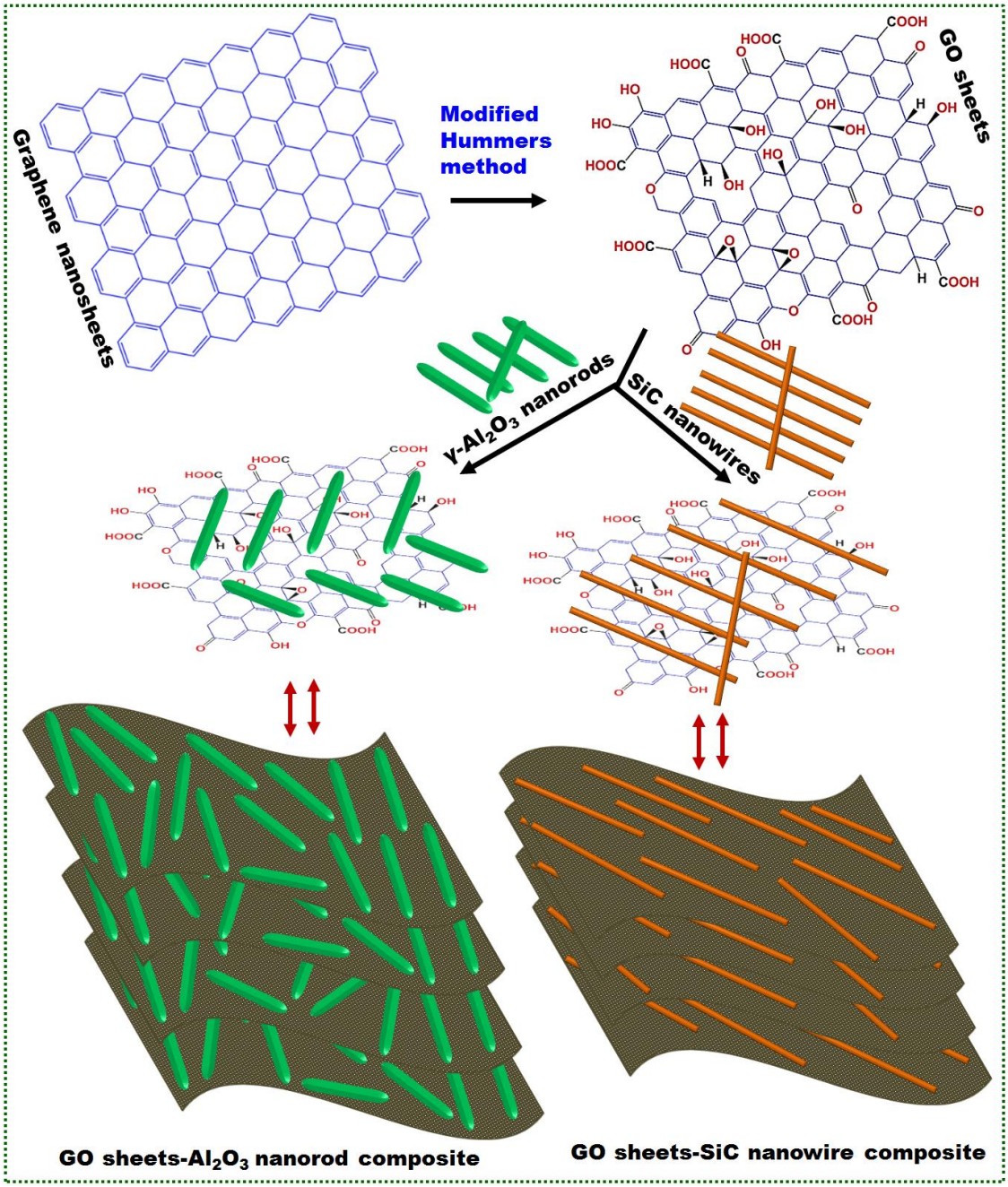

Figure 17. Design of GO-γ-Al_2O_3 nanorod as well as GO-SiC nanowires hybrid nanosheets. GO can be produced by graphene nanosheets by oxidation through a modified hummers' method. One-phase method is a simple technique to prepare these hybrid nanocomposites. These hybrids exhibit elevated surface area, ultrahigh robustness and physical features.